11.13 Heat-Assisted Machining

AKM Nurul Amin, International Islamic University Malaysia, Kuala Lumpur, Malaysia
TL Ginta, Universiti Teknologi, PETRONAS, Malaysia

11.13.1 Introduction

Heat-assisted machining or hot machining, as it is more popularly known, has emerged as an alternative method of machining providing improved machinability of difficult-to-cut metals and alloys. This technique of machining has been under consideration since the late nineteenth century. It was observed that metals tend to deform more easily when heated, thus enhancing their machinability. Hot machining found widespread application in the manufacture of engineering components in the late twentieth century, a century after it was first introduced. The principle behind hot machining is to increase the difference in hardness of the cutting tool and workpiece, leading also to the reduction in the component forces, improvement in surface finish, and longer tool life.

The manufacturing industry has explored various heating techniques such as electric current, arc, high-frequency induction, laser beam, electron beam, and plasma jet heating. However, all of these techniques are suitable for some but unsuitable for other specific operations. For instance, electron beam heating, requiring a vacuum for operation, was found to be expensive for machining applications, though the process can be successfully applied for cutting thick layer of metal with minimum metal losses and high quality of the generated surfaces. Laser heating, on the other hand, was found to be suitable for both cutting and machining applications. Laser is suitable for metals and nonmetals, such as ceramics. Laser can be customized for turning as well as milling, including micromilling applications because of the high flexibility of the focused beam. But when intended to be applied for bulk milling, such as end milling with a large-diameter tool intended for rough machining, the laser beam needs to be defocused to a wider area that requires a high-power laser to heat up the removable layer of material. Furthermore, the heating efficiency of the laser and the reflectivity of the laser beam are some of the additional problems in laser-assisted machining (LAM). Apart from that, the high costs of high-powered lasers (for example, a 1.5 kW CO_2 laser costs more than $150 000) and the large power consumption slowed down implementation of LAM (*1*).

Plasma-enhanced machining (PEM) has emerged as an economical alternative to LAM and has received significant attention in Germany. Machining experiments performed using PCBN tool inserts in turning ceramics showed that relief face tool wear was reduced by 40%. PEM was also used in turning extremely hard metals with tungsten carbide inserts. Although PEM is found to improve the machining performance, there is no applicable protection to avoid the heat effect on the cutting edge. Furthermore, the notch wear of the tool is another problem associated with PEM (*2*). PEM has yet another limitation: It is not suitable for milling applications where the feed rate is low and intense heat would lead to melting of the work material.

Heat retained in the steel rolls after the hot rolling operation was used to achieve low cutting forces and high tool life. Researchers used the even furnace heating method to study the influence of heating temperature on various criteria of machinability of work materials. In the early 1980s, Talantov et al. (*3*) and Amin and Talantov (*4*) studied the influence of the furnace heating method of workpiece on the machinability of carbon steel, stainless steel, and titanium alloy. They found substantial reduction in the tool wear rate and chatter when heating was employed. However, the researchers used the furnace method only to demonstrate the effect of heating the work material on the machinability of the materials since the furnace heating method is definitely not recommended for application in production.

Induction heating is a long method that is very efficient in terms of heat efficiency, and the cleanliness of the operation itself is very conducive for surface-hardening operation of metals. The industry has seen many diversified applications of induction heat-assisted quenching operation wide included in the manufacturing transfer lines as the final operation on parts after the machining operations. The short heating time practically leads to no rusting of the part, and thus it does not call for grinding needs. Amin and Abdelgadir showed the creativity of using induction heating for online heating of a thin layer of the workpiece immediately prior to the end milling process to improve the machinability of the material (*5*). Amin and his team conducted many research studies on heat-assisted machining using the new heating method. Amin and Abdelgadir (*6*) showed that induction heat-assisted machining was able to suppress chatter by 98% and to increase tool life severalfold in the case of steel. Amin et al. (*7*) conducted research on the influence of heating temperature (using the same heating method) on the performance of circular carbide inserts in the end milling of carbon steel. They concluded that the online workpiece heating could help in substantially reducing the acceleration amplitude of chatter, as well as in appreciably lowering average surface roughness and tool wear values. In another work, Amin et al. (*8*) used induction heat-assisted machining method to improve the machinability of Ti–6Al–4V alloy. They conducted the research on the use of online heating during machining of Ti–6Al–4V. This method of heating was found to result in a reduction in amplitude of chip serration and the formation of thicker chips leading to an increase in chip-tool contact length. Reduction of chatter amplitudes at resonance frequencies was due to the formation of stable chips and higher damping capacity from the side of the preheated workpiece. As a result, uniform tool wear with almost 2.5 times the reduction of average flank wear values was achieved. While the surface roughness was found to vary from 0.5 to 1.3 μm, with an increase in the cutting speed range from 40 to 160 m min^{-1} during normal room temperature machining, the same for heat-assisted machining was found to be approximately 0.2 μm in the same cutting speed range. The surface roughness value thus achieved after heat-assisted machining was low enough to suggest the elimination of the fine grinding and rough polishing operations.

Therefore, it can be concluded that induction heat-assisted machining is a good alternative to consider in vertical milling operations of difficult-to-cut metals and alloys. However, as mentioned earlier, this method is not suitable for turning operations, though some researchers have attempted to customize it for turning operations as well to designing the coil to be wrapped around the workpiece. However, this design is not universal enough to be recommended for all turning operations: The last part of the workpiece cannot be machined using such an arrangement of the coil because it would be obstructed by the rotation of the spindle.

11.13.2 Principles of Hot Machining

One way to improve the machinability of high-strength materials is through application of heat to the workpiece either immediately prior to or during machining. Highly intense local input of thermal energy by an appropriate heat source, as indicated in the previous section, drastically reduces the material strength when heated above some specific temperatures, depending on the properties of the work material. The softened metal is then easily removed by conventional cutting processes, such as turning and milling. Successful application of heat-assisted machining requires a localized and controlled heating of the material within the machining zone directly in front of the tool. A decisive precondition for success of hot machining is the decrease of material strength at elevated temperatures (*9*). According to investigations on conventional heating methods, a sufficient energy density on the workpiece is essential for the efficiency and feasibility of hot machining since otherwise the adequate material plastification could not be guaranteed due to fast heat conduction in milling (*10*) and heat convection in the case of turning operation due to the rotation of the workpiece at high speed. Investigations on the temperature-dependent material behavior revealed a significant loss of material strength above a certain temperature level for high-strength metal alloys (**Figure 1**). The application of intense laser radiation as a thermal tool was found to be one of the suitable heating methods in hot machining (*11,12*). Induction heating is another low-cost and clean method that is very suitable for milling operations (*13*) and arc heating in the case of turning (*14*).

The advantages of hot (heat-assisted) machining processes are reduced cutting forces, low tool wear, reduced chatter, and improved surface finish (*14*). The reduction of cutting and feed forces is associated with low shear yield strength of the work material at the primary and secondary shear planes. During hot machining, the plasticity of the work material increases, leading to increased chip-tool contact length, which plays a role in reducing the normal stress acting on the tool. Heating also reduces the intensity of chip serration, facilitating lower fluctuations of the cutting forces which lowers the dynamic stresses applied to the tool, thereby facilitating lower tool wear in heat-assisted machining.

Reduction of the intensity of chatter is associated with the increased internal damping of the system due to the increased plasticity of the work material, which absorbs the energy of the vibrating tool and dampens the vibration. Depending on the material properties, various degrees of damping are achieved during heat-assisted machining. The machined surface is improved for two reasons: lower amplitude of chatter and improved flow of the material over the rake and flank surfaces of the tool forming the two new surfaces. In machining, surface finish is known to be improved as a result of increases in cutting speed since higher cutting temperatures are generated during machining at higher cutting speeds, facilitating easy shearing and flow of the chip and machined surfaces as it also occurs in heat-assisted machining.

11.13.3 Brief Overview of PEM

11.13.3.1 Background

Many feasibility studies have been conducted over the past years with the use of intense heat to locally soften the work material prior to machining in an attempt to improve the machinability of difficult-to-cut materials. PEM is one of the most promising techniques that has been developed because it can provide the necessary heat intensities required to soften the workpiece, especially in turning, where high intensity is an essential requirement. Despite the earlier sign of its potentials, the high cost of high-power lasers

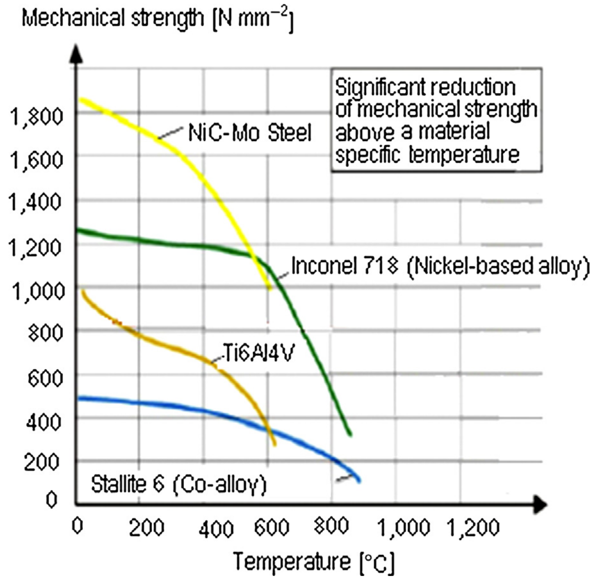

Figure 1 Temperature-dependent mechanical properties of high-strength metal alloys. Reproduced from Brecher, C.; Rosen, C. J.; Emonts, M. Laser-Assisted Milling of Advanced Materials. *Phys. Procedia* **2010,** *5*, 259–272.

prevented LAM from being widely adopted by industry. Plasma-assisted machining is found to be an economic alternative to LAM. PEM can offer comparable heating rates to lasers at much lower cost. For adopting PEM for industrial applications, its characteristics must be fully understood in order to achieve optimal machining conditions.

The ability to generate and transfer the desired degree of localized heating to the workpiece is critical to the success of PEM. Workpiece temperature plays an important role in the chip formation during the metal-cutting process as it affects the material deformation. The large amount of energy generated due to the bulk deformation and friction is almost exclusively converted to thermal energy, leading to high chip and tool-cutting temperatures. Temperature in the workpiece is especially important when thermally enhanced machining is used. The effects of externally applied heat sources on the temperature distribution of the workpiece must be known. Peak temperatures must be known so that thermal damage is prevented or minimized in the workpiece surface, and the temperature must be known at the cutting point to control the process.

11.13.3.2 Principle

By applying a plasma arc to soften a workpiece zone just in front of the cutting tool, very-high-energy densities are realized and the heat is confined. A plasma arc consists of a high-velocity, high-temperature stream of ionized gas capable of supporting a high-current, low-voltage electric arc. A plasma torch produces this phenomenon by having a tungsten electrode centrally placed within a water-cooled copper nozzle. A gas stream is fed down the annulus between these, the gas being ionized by a high-frequency discharge between the copper nozzle and the central electrode. This is followed by a low-current pilot arc and then by a high-current main arc. The arc characteristics and reliability of arc striking are improved with the balanced geometry of the nozzle orifice (*15*).

Heating in PEM is provided by direct current (dc), transferred arcs that generate thermal or equilibrium plasmas. Thermal arc plasma generators consist of a thoriated tungsten cathode and a cooled nozzle through which the plasma gas flows (Figure 2). The nozzle serves as anode when used with nonconducting workpieces, but, with conducting materials, the arc is transferred to the workpiece, which works as the anode. Fiber-optic radiation thermometers are capable of measuring surface temperatures with a desired range and target emissivity from up to 1.0, with the probe head providing a suitable target size that can be positioned on the cutting surface between the plasma nozzle and the cutting tool. With highly localized energy available at low gas-flow rates, transfer arcs are well suited to PEM of electrically conducting superalloys, with typical plasma peak temperature reaching 16 000 K.

Carl et al. (*15*), in their experimental evaluation of PEM performed on a PEM system, conducted turning using a plasma heating system. The plasma torch was fitted with a copper nozzle of 3.18 mm orifice diameter. Thoriated tungsten cathodes with a 20° included angle were used throughout the experiments. Various measurements were performed in-process and offline the performance of hot turning, applying the given heating method.

11.13.3.3 Advantages of Plasma Arc Hot Machining

Carl et al. (*15*) found that the benefits of PEM are demonstrated through the reduction of cutting forces and improved surface roughness over a wide range of cutting conditions. Madhavulu and Ahmed (*16*) observed in their work that the major advantages of the plasma-assisted turning process are increased metal removal rates, lower spindle power requirement, and possibility of machining hard and tough metals even when fully hardened and heat treated. The results from their tests conducted on stainless steel indicated that hot machining leads to a 1.8 times gain in metal removal rate and a 1.67 times improvement in tool life. They observed, however, that, in hot machining the sum of the power required by the machine tool and the plasma heating system is far larger than the power required for the machine tool in the conventional machining process. But from their cost analysis, they found that the cost of power was much smaller than the savings in tooling cost and the overall machining cost due to lower lead time and higher productivity.

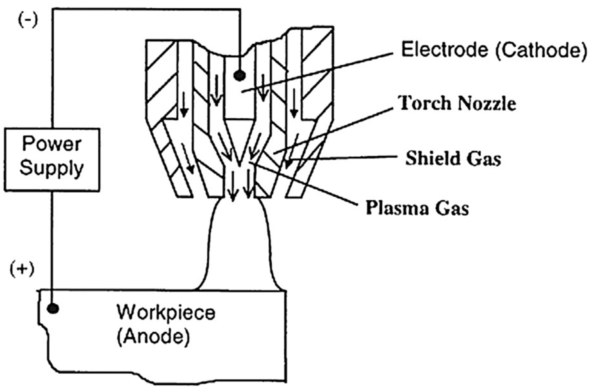

Figure 2 Details of a plasma arc (transferred arc) generator. Reproduced from Sun, S.; Harris, J.; Brandt, M. Parametric Investigation of Laser-Assisted Machining of Commercially Pure Titanium. *Adv. Eng. Mater.* **2008,** *10*, 565–572.

11.13.4 Brief Overview of Laser-Assisted Machining (LAM)

Laser-assisted processing of material is one of the emerging fields in advanced manufacturing. The advantages that make the lasers increasingly attractive in industrial production include coherence, focus ability, very-high-power intensity, power-shaping capability, and ease of automation with in-process sensing (*17*). It also offers the potential to realize innovative design with high flexibility, a high processing speed, and good quality in many manufacturing processes. The capital investment may be higher, but this is offset by the benefits gained in many applications.

11.13.4.1 Principle of LAM Application in Turning

Application of laser beam heating in turning operations is relatively simple due to the stationary nature of the cutting tool (*18*). The variables in the laser beam are its position, spot size, incident angle, and tool to beam distance. The laser beam is placed normal to the workpiece surface in most of the reported work on laser-assisted turning operations (*19–23*), as indicated in **Figure 3**. This arrangement is sometimes preferred since machining is easy and the laser equipment does not come close to the machining area, but the heating efficiency of the machined surface is poor in this case and is not high enough deep for cut. The other alternative used by many researchers (*24–26*) is to place the laser gun incident normal to the cutting (chamfer) surface (as shown in **Figure 4**). The laser spot size is required to fully cover the chamfer surface in order to achieve uniform reduction in the cutting forces in the *x*-, *y*-, and *z*-directions (*26*). However, even partial coverage of the chamfer surface by the laser beam close to the machined surface can dramatically reduce tool wear (*27*).

Shin and colleagues (*28,29*) used multiple distributed laser units, simultaneously heating both the unmachined surface and the chamfer surface (**Figure 5**) to create the desired temperature distribution through the depth of cut in the workpiece, which is

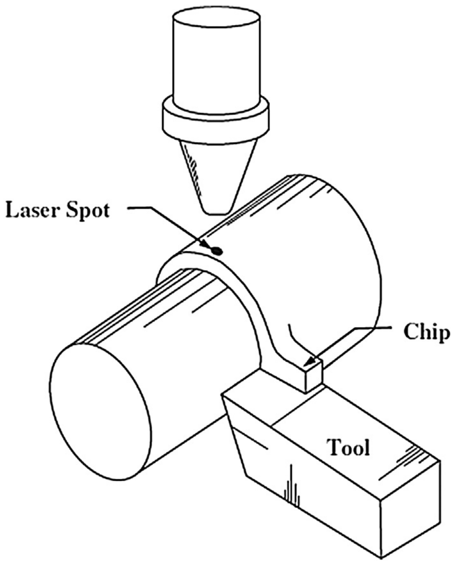

Figure 3 LAM setup with the laser beam normal to the workpiece surface. Reproduced from Wu, J. F.; Guu, Y. B. Laser Assisted Machining Methods and Device, US Patent 7,002,100 B2, 2004.

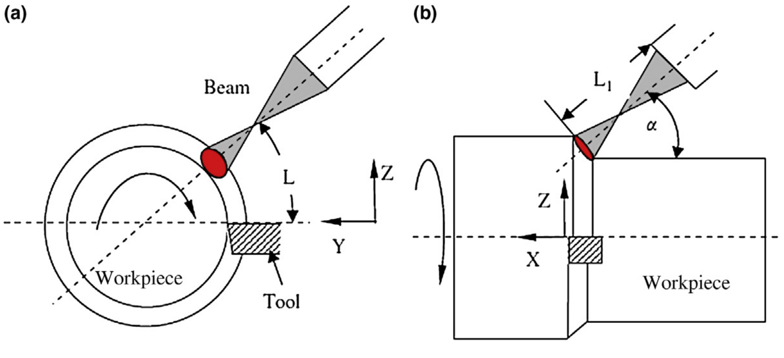

Figure 4 The relative position of the laser beam, workpiece, and cutting tool in laser-assisted turning operation: (a) End-view; (b) Side view. Reproduced from Sun, S.; Harris, J.; Brandt, M. Parametric Investigation of Laser-Assisted Machining of Commercially Pure Titanium. *Adv. Eng. Mater.* **2008,** *10*, 565–572.

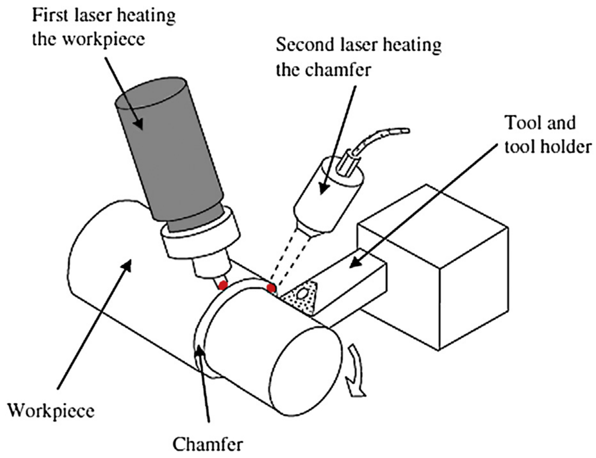

Figure 5 Laser-assisted turning utilizing two laser beams. Reproduced from Shin, Y.C. Laser Assisted Machining Process with Distributed Lasers. US Patent 0062920A1, 2007.

reported to result in longer tool life. The position of the laser beam relative to the tool is critical. Tool–beam distance, along with cutting speed, determines the time interval between the laser heating and machining operation and hence the temperature distribution at the cutting zone. It is found that the larger reduction in the cutting forces is achieved with the laser spot positioned closer to the cutting tool when cutting hardened steel (*30*), commercially pure titanium (*26*), and high chromium white cast iron (*31*). However, if the tool–beam is too close to the tool, machining problems may result (*32*). Therefore, the tool must be kept at a minimum distance from the laser beam.

11.13.4.2 Principle of LAM Application in Milling

Milling integration of the laser beam with a milling machine as the tool is rotating is a complicated task. Generally, the beam can be arranged separately from the tool or integrated with the spindle. For surface milling, the easiest way is to set the beam in front of the tool in the feed direction as shown in Figure 6. The limited spot size of the external heat source limits the ability to cover the width of cut by a single spot in most applications. Therefore, the beam can only heat part of the cut width. This could be the middle (position 1) (*33*) or tool entry point (position 2), or both entry and exit points (position 2 and position 3) by two beams (*34,35*). A high-power laser, multiple beams, or a line beam are required to cover the width of the cutting zone (region 4) (*35–38*). The dynamic impact on the cutting tool, as the rotating tool intermittently engages and disengages with the workpiece at the entry and exit points, respectively, causes significant vibration and ultimately tool fracture during milling operations. As a result, laser beam heating at the entry point is more significant for longer tool life and a reduction in chatter. Rajagopal et al., (*25*) experimenting with a 14 kW CO_2 laser on titanium and Inconel 718, showed that beam location is important during LAM. Various coatings were studied, including India ink, silicon carbide, and potassium silicate, with varying degrees of successful absorptivity enhancement.

11.13.4.3 Benefits of LAM

Komenduri et al. (*39*) conducted research on LAM of Ti–6Al–4V and Inconel 718 using an Nd–YAG pulse laser, which has the advantage of providing higher absorptivity for metals due to its shorter wavelength. To overcome the intermittent energy problem, two different techniques were applied. First, Komenduri used the laser as a primary heat source at a high pulse rate and observed

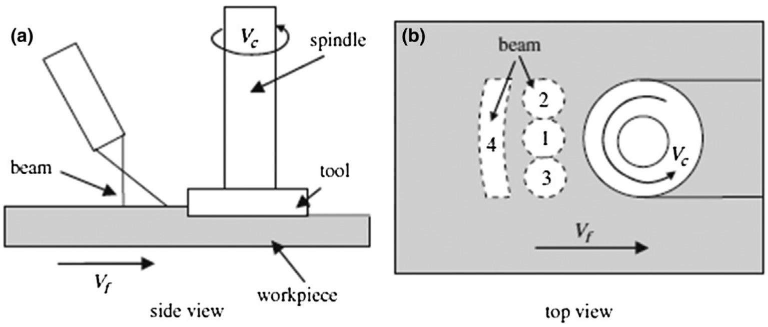

Figure 6 Illustration of the integration of the beam with the cutting tool for surface milling. Reproduced from Sun, S.; Harris, J.; Brandt, M. Parametric Investigation of Laser-Assisted Machining of Commercially Pure Titanium. *Adv. Eng. Mater.* **2008,** 10, 565–572.

a 49% reduction in cutting forces and chip fragmentation during LAM of Inconel 718. For Ti–6Al–4V forces dropped by 30% in air and 60% with oxygen assistance. Second, he used the laser to precondition the workpiece before machining and obtained a 28% reduction in forces for Ti–6Al–4V. However, it lacked any detailed analysis, no improvements in tool wear were reported, and surface roughness was observed.

Several researchers have investigated advanced ceramics in a thermally assisted turning operation. For example, Copley (*1*), who applied a fillister-shaped removal mode to three-dimensional machining of Si_3N_4, pointed to the relation between the fillister shape and laser polarization. His results show that the strength of the Si_3N_4 after machining is about 30% greater than that produced by conventional diamond grinding. Copley also proposed the application of a slanted laser to heat materials at the same time that a single-point cutting tool is removing the material by lathe. This method did increase the material removal rate and tool life but was thought to suit only metal materials. In their search for a new ceramics cutting technique, Uehara and Takeshita (*12*) used hot machining to cut mullite and Si_3N_4 ceramics, measuring the outcomes in terms of cutting force, chip shape, surface roughness, and tool wear. The first successful use of LAM in machine ceramic material was by Konig and Zaboklicki (*40*), who obtained continuous chips for hot-pressed silicon nitride when its temperature exceeded 1200 1C. They applied LAM to both turning and milling ceramics and composites, and reported low cutting force, small tool wear, and a high material removal rate as characteristics. They found the surface roughness to be equal to that of a ground surface with R_a less than 0.5 μm. However, by not examining material-removal mechanisms and subsurface damage, this experiment neglected to collect information essential to the LAM process, namely, the effects of laser energy on workpiece temperature and the impact of temperature on tool wear. Chryssolouris (*41*) tested the application of LAM to general metals, heating the workpiece surface with a continuous laser beam before removing the material with a cutting tool. This experiment found a reduction in tool wear, with a cost reduction of 60–80% over the conventional grinding method.

11.13.5 Effect of Heating Temperature (in the Furnace Heating Method) on the Machinability of Materials

11.13.5.1 Experimental Methods

Furnace heating is not a practical heating method. Nevertheless, Amin (*42*) used this method in his study to investigate the influence of workpiece heating on chip serration, coefficient of chip shrinkage, chip-tool contact length, cutting force, and tool wear in turning. An induction furnace was used for the purpose. First, the workpiece was heated to a temperature approximately 50°°C above the required temperature to compensate for the loss of heat during the transfer of the workpiece from the furnace to the machine and clamping. Second, an auxiliary cutting tool, moving ahead of the main tool by 2–3 mm, was employed to remove the cooled outer skin (1–1.5 mm) of the workpiece, as shown in Figure 7. The inner temperature of the workpiece was measured using a thermocouple at the start and end of the experiment. The variation in the workpiece temperature was controlled within ±50 °C of the designed temperatures. Depth of cut and feed were maintained at 2 mm and 0.467 mm per rotation, respectively. Investigations were conducted for heat-resistant steel ЗИ 481 (Russian Grade) and titanium alloy–BT-3-1 (Russian Grade).

In order to study the frozen chip, the drop tool apparatus shown in Figure 8 was used. Optical microscopes were used to study the chip-tool samples and tool wear, and a 3-axis dynamometer was used for force measurement.

11.13.5.2 Effect of Heating Temperature on Chip-Tool Contact Length and Chip Shrinkage

The effects of heating temperature on the chip shrinkage coefficient and morphology of chip were studied. It was observed that with the increase in the heating temperature the coefficient of chip shrinkage and the chip-tool contact length increase at the beginning up to a particular temperature, specific to the optimum temperature of preheating, and then decline with further increase in

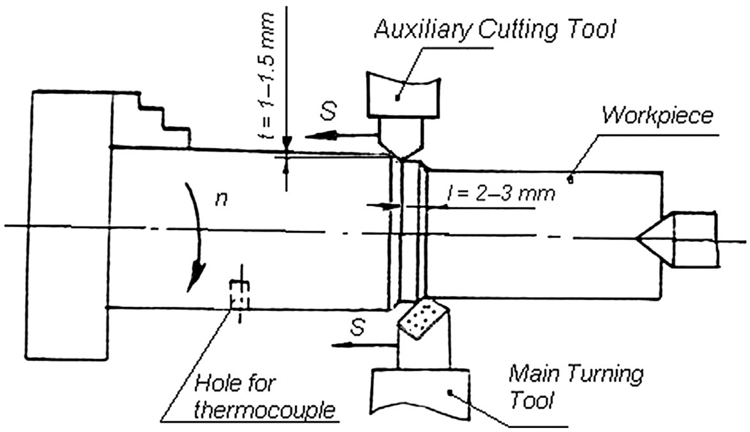

Figure 7 Arrangement of cutting after preheating in furnace. Reproduced from Amin, A. K. M. N. Investigation of the Laws Governing the Formation of Chatter during Metal Cutting Processes and their Influence on Tool Wear. Ph.D. Thesis (in Russian), Volgograd Polytechnic Institute, Volgograd, Russia, 1982.

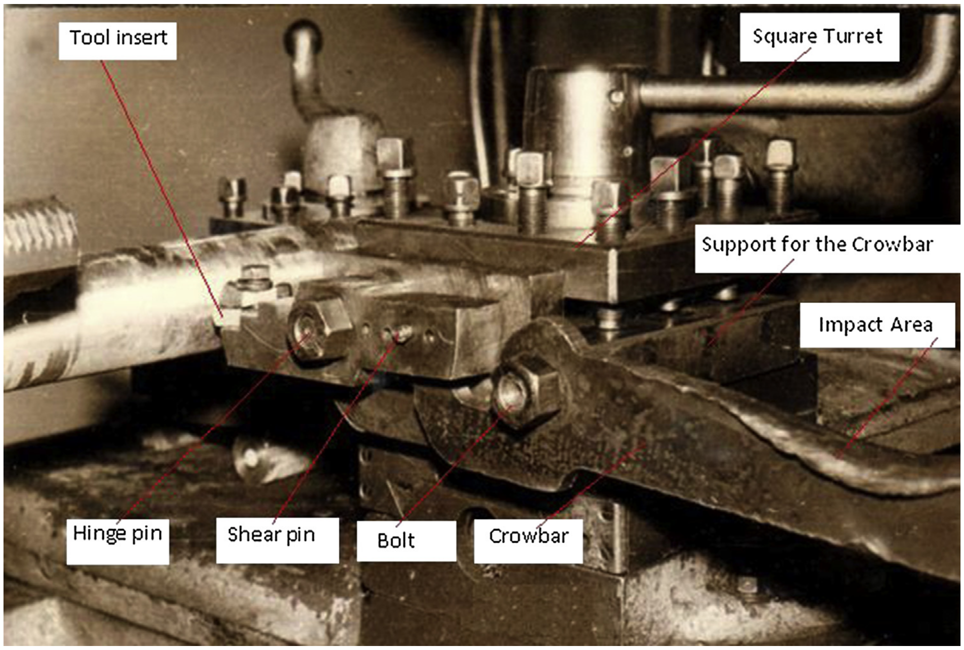

Figure 8 Drop tool apparatus for lathe application. Reproduced from Amin, A. K. M. N. Investigation of the Laws Governing the Formation of Chatter during Metal Cutting Processes and their Influence on Tool Wear. Ph.D. Thesis (in Russian), Volgograd Polytechnic Institute, Volgograd, Russia, 1982.

temperature (**Figure 9**). The optimum temperatures with the two values at the maximum were found to be 570 K (300 °C) and 770 K (500 °C) for heat-resistant steel ЗИ 481 and titanium alloy–BT-3-1, respectively (**Figure 9**). The increase in chip-tool contact length and coefficient of chip shrinkage is related to the increase in the ductility of the work material. However, as the heating temperature is further increased (beyond the optimum temperature), the temperature at the chip-tool interface increases, which leads to lower yield strength of the material at the flow zone. As a result, lower amounts of work are done at the rake face of the tool due to chip movement, resulting in a shift of the shear plane angle to higher values according to the minimum energy theory of metal cutting (*43*). At higher values of the shear angle, the chip starts to become thinner and the chip-tool contact length is reduced.

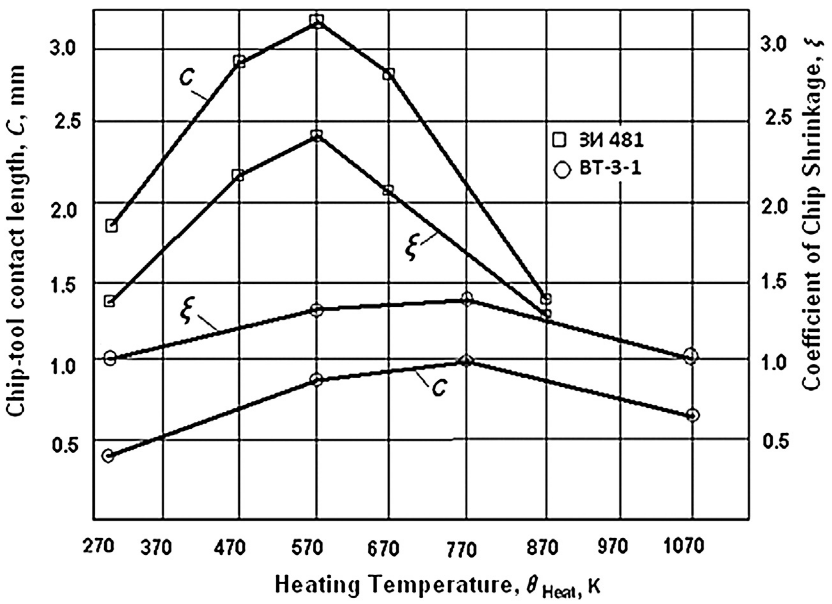

Figure 9 Dependence of chip-tool contact length, c and coefficient of chip shrinkage, ξ on workpiece heating temperature. Work materials: Heat-resistant steel ЗИ 481 (Russian Grade) and titanium alloy–BT-3-1 – (Russian Grade). Tool material: BK 8 (uncoated WC–Co tool with 8% carbon). Reproduced from Amin, A. K. M. N. Investigation of the Laws Governing the Formation of Chatter during Metal Cutting Processes and their Influence on Tool Wear. Ph.D. Thesis (in Russian), Volgograd Polytechnic Institute, Volgograd, Russia, 1982.

11.13.5.3 Effect of Heating Temperature on Cutting Force Components

The effect of workpiece heating temperature on the horizontal components of cutting force was investigated for both of the work materials. Figures 10(a)–10(c) shows the plot of the upper and lower levels of in-force components (P_z, P_y and P_x) versus heating temperature, θ_{heat} for titanium alloy BT-6, and Figures 11(a)–11(c) shows the same thing for heat-resistant steel ЗИ 481. As shown in Figures 10(b), 10(c), 11(b), and 11(c), the upper and lower levels of the horizontal components of cutting force P_y and P_x attain their maximum values at a particular temperature (570 K and 770 K for steel ЗИ 481 and titanium alloy–BT-3-1, respectively), specific to the material. The same phenomenon was observed in the cases of chip-tool contact length and coefficient of chip shrinkage. However, as also observed in Figures 10(a) and 11(a), in the case of the vertical (tangential) component of cutting force, F_z, a similar increase in cutting force at the specific temperature was not observed. On the contrary, a continuous decrease in the value of this component of cutting force with the increase in temperature was recorded.

It was further observed that the amplitude of vibration of cutting force (distance between the upper and lower boundaries of the cutting force curves) is very low at the optimum preheating temperature. The relatively high value of the horizontal cutting force components at the optimum temperature is related to the increased length of contact of the chip with the tool and the value of the coefficient of chip shrinkage, as discussed in the previous section.

11.13.5.4 Effect of Heating Temperature on Chip Serration

The chip root specimens were studied for room temperature and heat-assisted machining conditions. Two sample chip roots specimens for BT-3 are shown in Figures 10(a) and 10(b). Under the room temperature condition, the titanium alloy chips are

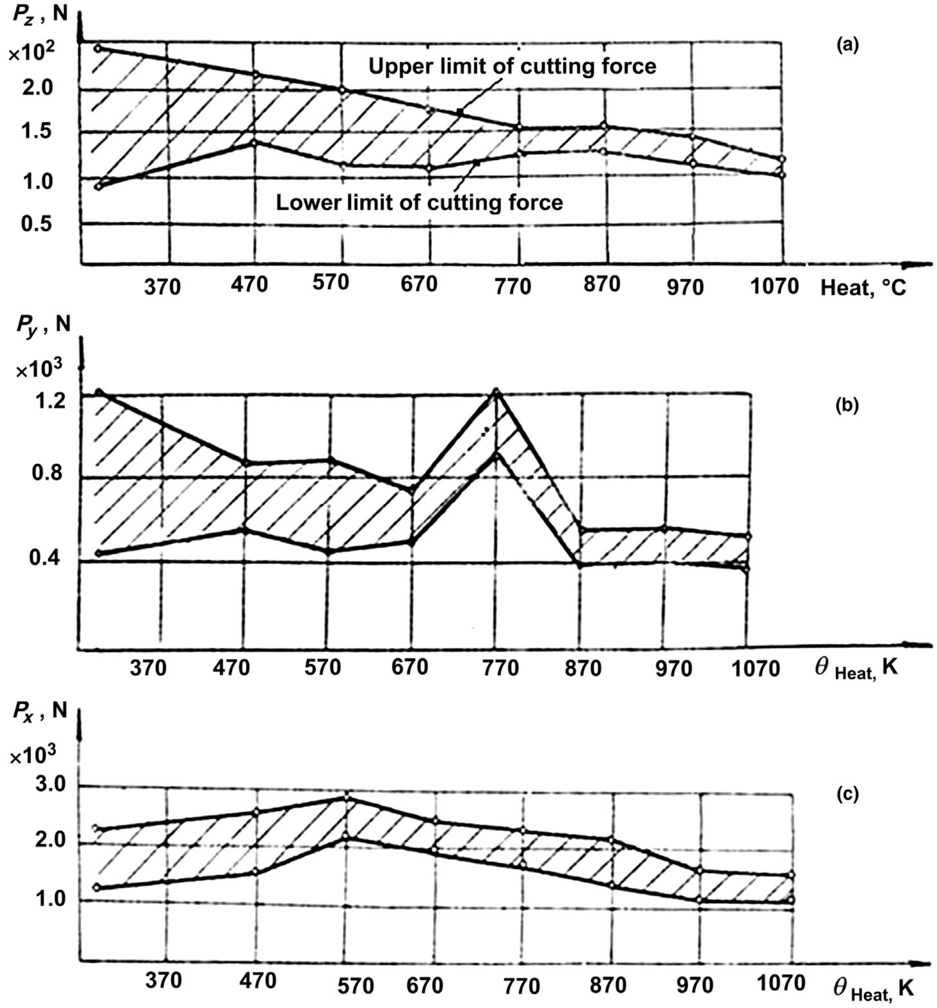

Figure 10 Dependence of horizontal components cutting force P_z, P_y, and P_x on workpiece heating temperature. Work materials: titanium alloy–BT-3-1 – (Russian Grade). Tool material: BK 8 (uncoated WC–Co tool with 8% carbon). Reproduced from Amin, A. K. M. N. Investigation of the Laws Governing the Formation of Chatter during Metal Cutting Processes and their Influence on Tool Wear. Ph.D. Thesis (in Russian), Volgograd Polytechnic Institute, Volgograd, Russia, 1982.

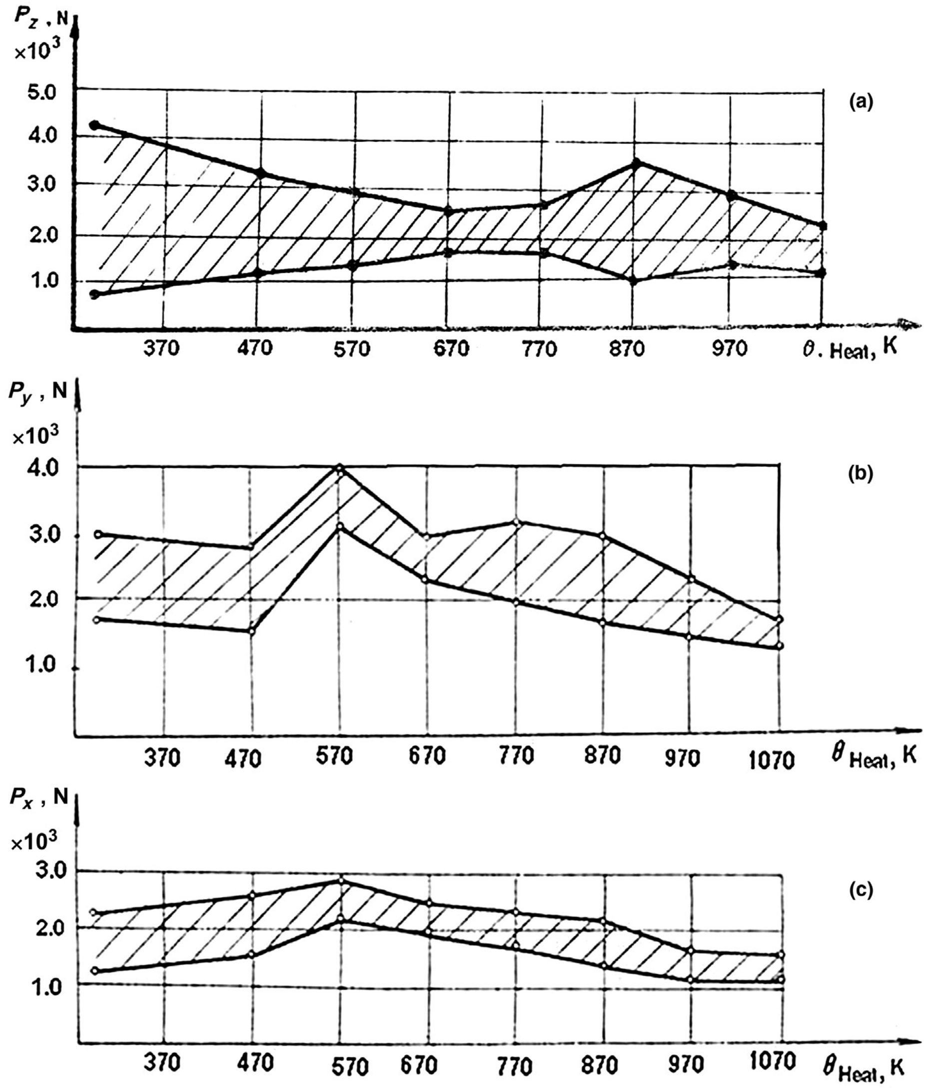

Figure 11 Dependence of horizontal components cutting force P_z, P_y, and P_x on workpiece heating temperature. Work materials: Heat-resistant steel ЭИ 481 (Russian Grade). Tool material: BK 8 (uncoated WC–Co tool with 8% carbon). Reproduced from Amin, A. K. M. N. Investigation of the Laws Governing the Formation of Chatter during Metal Cutting Processes and their Influence on Tool Wear. Ph.D. Thesis (in Russian), Volgograd Polytechnic Institute, Volgograd, Russia, 1982.

highly serrated. But at the critical heating temperature (Figures 7, 8(b), and 8(c)), the chip serration is greatly reduced. Chip serration amplitude was greatly reduced, and almost continuous chips were formed at the critical temperature in the case of titanium alloy–BT-3-1, though titanium chips are entirely serrated in machining under room temperature condition (Figure 12(a)). However, in the case of heat-resistant steel ЭИ 481, chip serration could be entirely eliminated (*42*).

11.13.5.5 Effect of Heating Temperature on Tool Wear

The effect of heating temperature on average flank wear is shown in Figures 13(a) and 13(b) for titanium alloy–BT-3-1 and heat-resistant steel ЭИ 481, respectively. These two figures show that flank wear is lowest at the corresponding critical heating temperatures for the two materials (770 K for BT-3-1 and 570 for ЭИ 481). Hence the critical temperature can be termed the optimum heating temperature.

Reduction of average tool wear at this temperature is related to lower stresses of the tool as a result of increased chip-tool contact length and less intense chatter due to the formation of more stable chips. In addition, the initial wear is minimal at the optimum heating temperature for both materials due to the effect of lower dynamic stresses on the tool and the lower yield strength on the work material at the higher heating temperatures. However, at the temperature above the optimum value, initial wear along with the average value of the flank wear increases due to higher rates of diffusion wear at the elevated temperature.

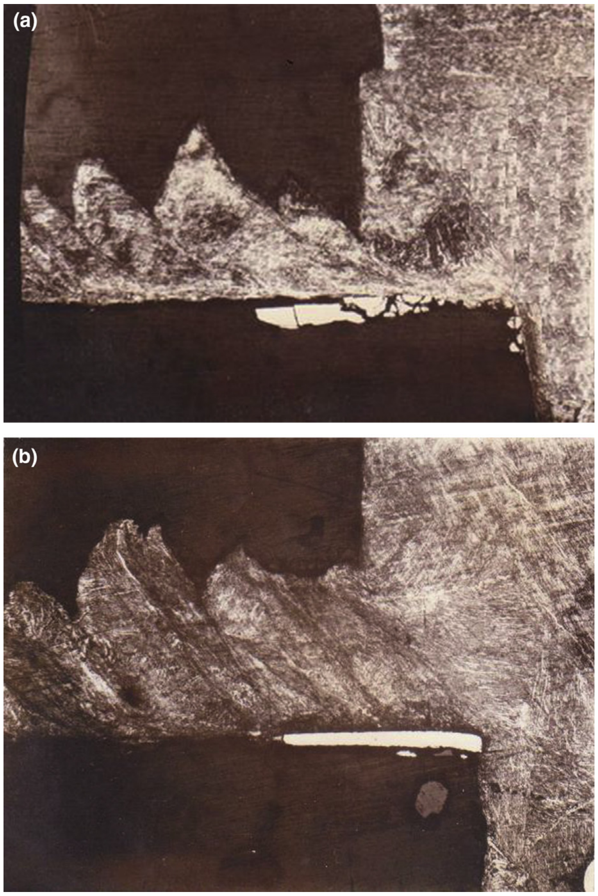

Figure 12 Influence of workpiece heating on chip serration. Work materials: titanium alloy–BT-3-1 – (Russian Grade). Tool material: BK 8 (uncoated WC–Co tool with 8% carbon). Reproduced from Amin, A. K. M. N. Investigation of the Laws Governing the Formation of Chatter during Metal Cutting Processes and their Influence on Tool Wear. Ph.D. Thesis (in Russian), Volgograd Polytechnic Institute, Volgograd, Russia, 1982.

The reduction in flank wear observed after equal amounts of machining time is approximately five times in the case of BT-3-1 and 4.5 times in the case of ЗИ 481.

11.13.5.5.1 Effect of Heating Temperature on Tool Wear during Turning of BT-3-1

Views of the tool rake and flank faces after 360 s of machining under dry room temperature conditions, at the optimum cutting temperature and a higher temperature, are shown in Figures 8, 12, 13, and 14 for titanium alloy–BT-3-1. Figures 8–12 shows that under room temperature conditions, the wear intensity is high and failure of the tool is caused mainly by brittle failure modes. It may be related to high chip serration amplitude and dynamic loading on a small chip-tool contact area, specific for titanium alloys. Figures 14(a) and 14(b) demonstrated that the contact length in room temperature machining was only 0.5 mm (approximately).

At the optimum temperature, the tool wear was very nominal at both the flank and the rake faces (Figure 15). The contact length is approximately doubled compared to that under room temperature conditions. The low-wear intensity and uniform wear of the rake and flank surfaces of the tool were due to the beneficial role of heat-assisted machining in terms of lower chatter amplitude, lower dynamic loading on the tool, and increased chip-tool contact length.

At the 1070 K ($\approx$800 °C) temperature, tool wear was very smooth at both the flank and rake faces (Figure 16) due to the diffusion mechanism of wear. However, the wear intensity was much higher and the chip-tool contact length much smaller compared to that at optimum temperature conditions. This relatively low and uniform wear compared to that at room temperature condition is again due to the beneficial role of heat-assisted machining in terms of lower chatter amplitude and lower dynamic loading on the tool.

It may therefore be concluded that there is a particular heating temperature for a given work material, the so-called optimum heating temperature, which when applied during machining improves the overall machinability of the work material, in terms of cutting force, tool wear/tool life, and chatter. Heating above the optimum temperature leads to higher tool wear/lower tool life due to excessive heat generation and higher rate of diffusion wear and superficial plastic deformation mechanisms.

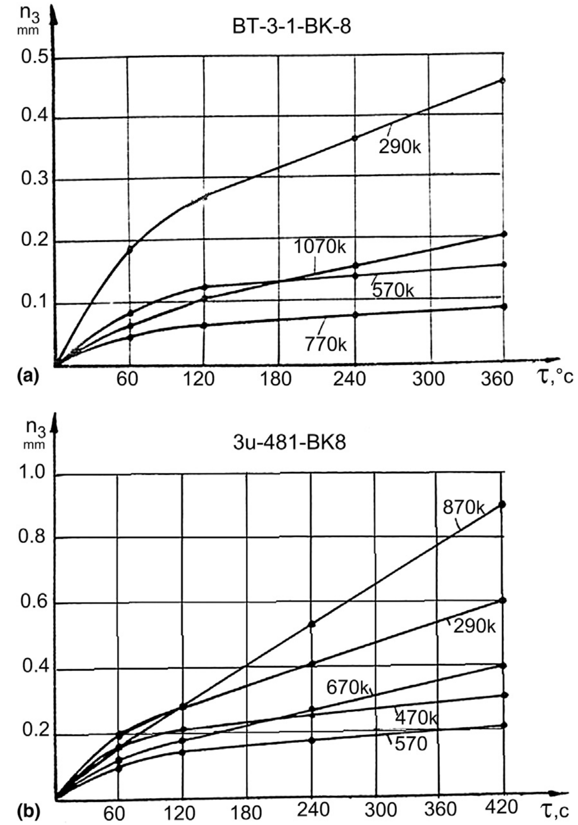

Figure 13 Dependence of average tool flank wear on cutting time for different workpiece heating temperatures: (a) For titanium alloy–BT-3-1; (b) Heat-resistant steel ЗИ 481. Tool material: BK 8 (WC–Co tool with 8% carbon). Reproduced from Amin, A. K. M. N. Investigation of the Laws Governing the Formation of Chatter during Metal Cutting Processes and their Influence on Tool Wear. Ph.D. Thesis (in Russian), Volgograd Polytechnic Institute, Volgograd, Russia, 1982.

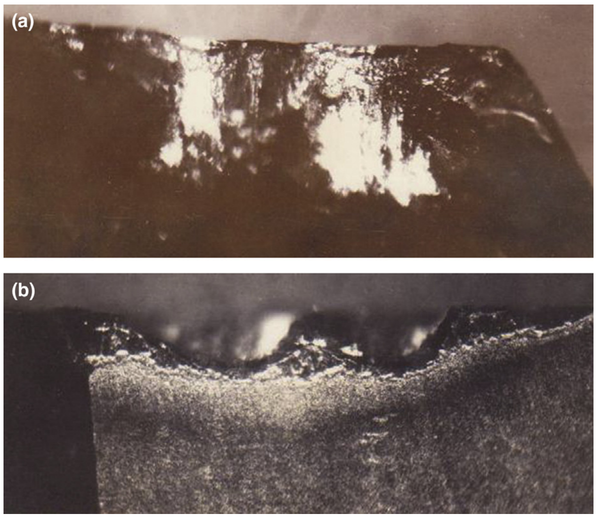

Figure 14 Views of the rake face (a) and the flank surface (b) of the tool for titanium alloy–BT-3-1 – (Russian Grade) after 360 s of machining under dry room temperature condition. Tool material: BK 8 (WC–Co tool with 8% carbon). Reproduced from Amin, A. K. M. N. Investigation of the Laws Governing the Formation of Chatter during Metal Cutting Processes and their Influence on Tool Wear. Ph.D. Thesis (in Russian), Volgograd Polytechnic Institute, Volgograd, Russia, 1982.

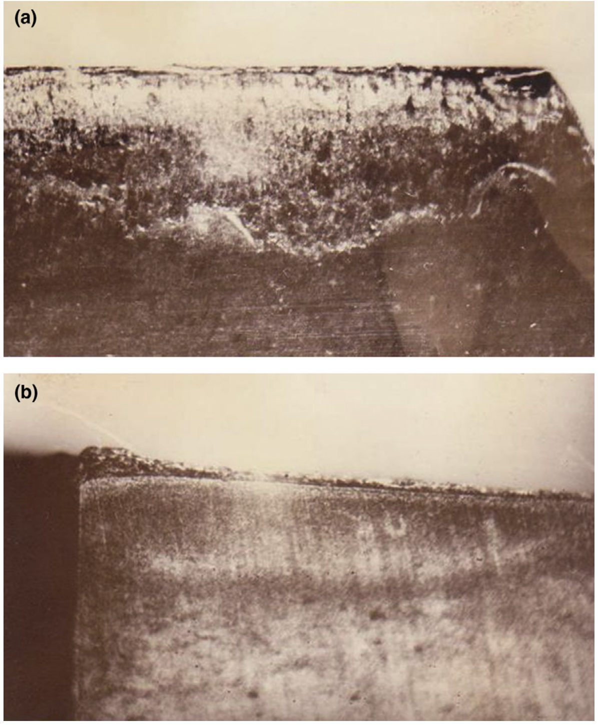

Figure 15 Views of the rake face (a) and the flank surface (b) of the tool for titanium alloy–BT-3-1 – (Russian Grade) after 360 s of machining under heat-assisted condition at the optimum heating temperature of 770 K. Tool material: BK 8 (WC–Co tool with 8% carbon). Reproduced from Amin, A. K. M. N. Investigation of the Laws Governing the Formation of Chatter during Metal Cutting Processes and their Influence on Tool Wear. Ph.D. Thesis (in Russian), Volgograd Polytechnic Institute, Volgograd, Russia, 1982.

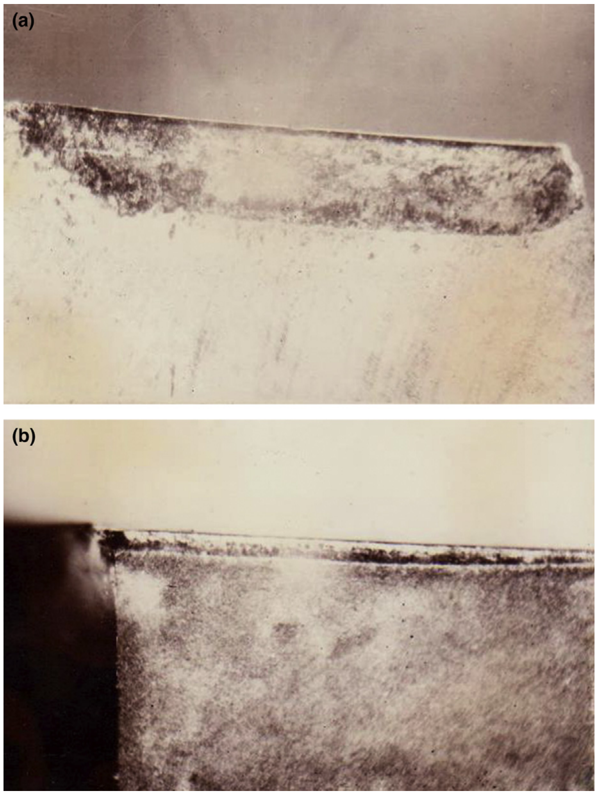

Figure 16 Views of the rake face (a) and the flank surface (b) of the tool for titanium alloy–BT-3-1 – (Russian Grade) after 360 s of machining under heat assisted condition at the highest applied heating temperature of 1070 K. Tool material: BK 8 (WC–Co tool with 8% carbon). Reproduced from Amin, A. K. M. N. Investigation of the Laws Governing the Formation of Chatter during Metal Cutting Processes and their Influence on Tool Wear. Ph.D. Thesis (in Russian), Volgograd Polytechnic Institute, Volgograd, Russia, 1982.

11.13.6 Induction Heat-Assisted Machining Applied to End Milling

11.13.6.1 Method of Heating and Process Parameter Control

End milling tests were conducted on a Vertical Machining Center (VMC ZPS, Model: MCFV 1060 LR). Figure 17 shows a block diagram of the experimental setup.

11.13.6.2 Induction Heating Equipment

Induction heaters provide alternating electric current to an electric coil (the induction coil), as a result of which the induction coil becomes the electrical (heat) source that induces a high-frequency alternating electrical current into the workpiece to be heated. No contact is required between the workpiece and the induction coil acting as the heat source, and the heat is restricted to localized areas or surface zones immediately adjacent to the coil. This happens because the alternating current (ac) in an induction coil has an invisible force field (or magnetic flux) around it. When the coil is placed next to the tool approximately 5 mm above the workpiece surface, the lines of force concentrate in the air gap between the coil and the workpiece. The induction coil actually functions as a primary transformer, with the workpiece to be heated becoming the secondary transformer. The force field surrounding the induction coil induces an equal and opposing alternating electric current in the workpiece, with the workpiece then heating due to the resistance to the flow of this induced high-frequency alternating electric current. The rate of heating the workpiece is dependent on the frequency and intensity of the induced current, the specific heat of the material, the magnetic permeability of the material, and the resistance of the material to the flow of current. The induced currents are sometimes referred to as *eddy currents*, with the highest intensity current being produced within the area of the intense magnetic fields.

To heat the workpiece, a Portable Transistor Induction Heating Machine SP-25AB (25 kW capacity) and GP-35AB (25 kW capacity) were used for steel and titanium alloy Ti–6Al–4V, respectively. In the present study, a portable high-frequency inducting heating equipment was used for preheating the work material just prior to machining with the heating coil placed ahead of the cutting tool. This high-frequency current with alternative polarity generates *eddy currents* in the surface layer of the workpiece to heat up the layer.

This process has numerous advantages over other heating methods since the generated electric current is simpler to control than other processes. The heating system consists of three major components (Figure 18): high frequency transformer (Invertors), Matching Box (Transformer and Condenser), and cooling unit (designed for industrial use).

11.13.6.3 Cutting Force Measurement

The Kistler Rotating Cutting Force Dynamometer was used for measuring cutting forces. The complete measuring system consists of rotor (type 9125A), stator (type 5235), connecting cable (type 1500A37), and signal conditioner (5267A1/A2). The setup for the cutting force measurement is presented in Figure 19. The computer software used is Kistler DynoWare (type: 2825D1-2, version 2.31), which is a universal and operator-friendly software. The instrument can measure two components of cutting force: thrust force for along the *z*-axis (F_z) in N and cutting torque along the *z*-axis (M_z) in Nm.

11.13.6.4 Data Acquisition System for Vibration/Chatter and Temperature Monitoring

The data acquisition system includes vibration sensors, thermocouples, and a transducer. The transducer was connected to the computer via an interface card. Figure 15 shows a block diagram of the experimental setup. A photograph of the data acquisition

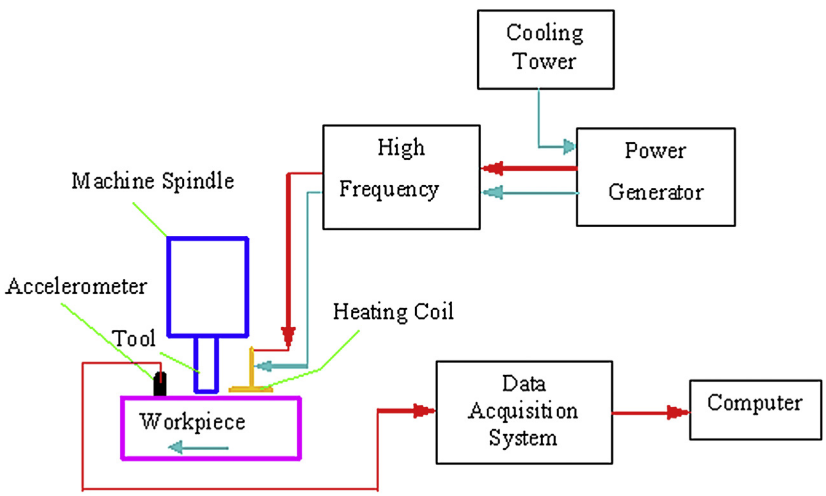

Figure 17 Experimental setup. Reproduced from Turnad, L. G. Improvement of Machinability of Titanium Alloy Ti-6Al-4V through Workpiece Preheating. Ph.D. Thesis, Manufacturing and Materials Engineering Department, IIUM, Malaysia, 2009.

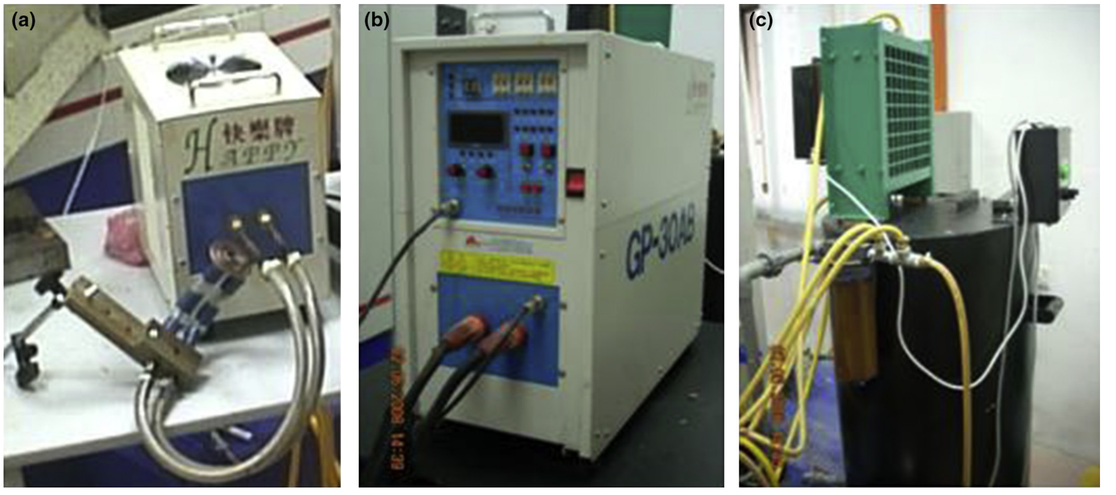

Figure 18 Portable transistor induction heating machine GP-30AB. (a) High-frequency transformer (Invertors); (b) Matching box (transformer and condenser); (c) Cooling unit (specially designed). Reproduced from Turnad, L. G. Improvement of Machinability of Titanium Alloy Ti-6Al-4V through Workpiece Preheating. Ph.D. Thesis, Manufacturing and Materials Engineering Department, IIUM, Malaysia, 2009.

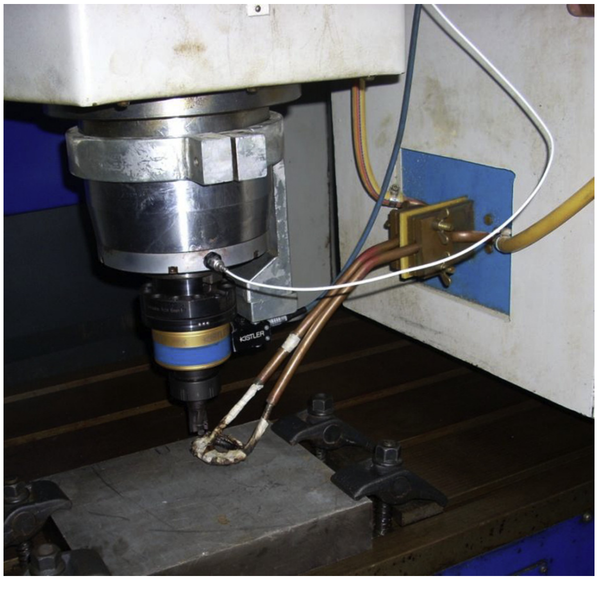

Figure 19 Cutting force measurement, vibration sensor, and coil induction heating setup 9. Reproduced from Turnad, L. G. Improvement of Machinability of Titanium Alloy Ti-6Al-4V through Workpiece Preheating. Ph.D. Thesis, Manufacturing and Materials Engineering Department, IIUM, Malaysia, 2009.

system is shown in Figure 20. As with any data acquisition system, the hardware of the system needs to be programmed by software. A customized version of LABVIEW software called DASYLab5.6 was used. DASYLab5.6 stands for Data Acquisition System Laboratory. In the data acquisition program the data are sent as data blocks via connections (data channels) between the single modules, so DASYLab works in a block-dependent mode. Each module output has a 64-kbyte buffer to hold the processed data.

The sensor attached to the vibrating system sends the signal to the computer through the signal conditioning module and the interface card. Throughout this research, DASYLab5.6 software was used to collect, simulate, and analyze the data (vibration signal and temperature).

11.13.6.5 Cutting Tools and Workpiece Materials

11.13.6.5.1 Cutting Tools

The inserts chosen for this study were Sandvik uncoated tungsten carbide-cobalt (WC–Co), inserts of the shape shown in Figure 21. The shape and geometry of the cutting tools are illustrated in Table 1. The inserts were fitted on a 20-mm-diameter Sandvik End mills tool holder.

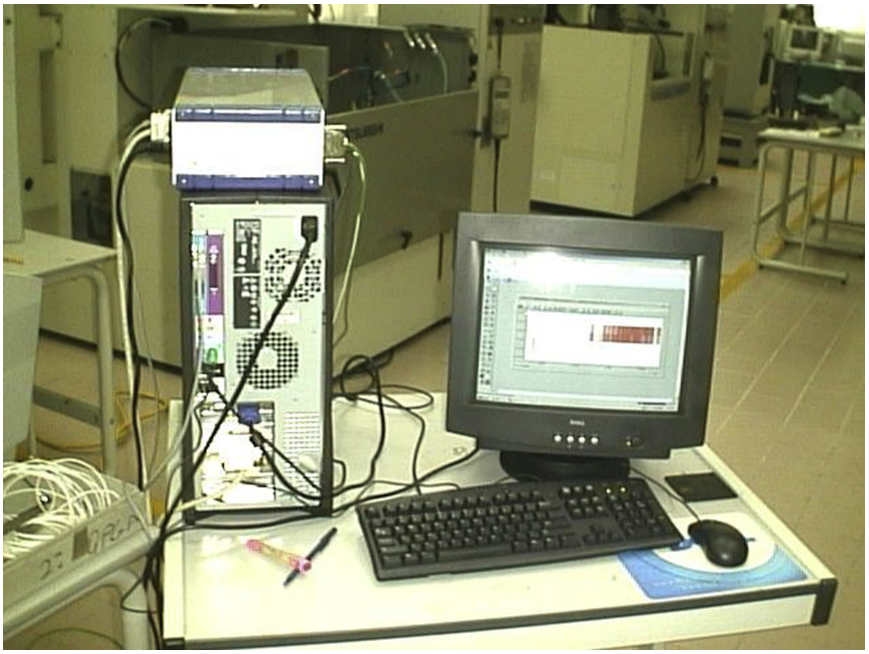

Figure 20 Data acquisition system. Reproduced from Amin, A. K. M. N.; Abdelgadir, M. The Effect of Preheating of Work Material on Improved Machinability of Materials. In *Proceedings of the International Conference AIMTDR*, Ranchi, India, 2002.

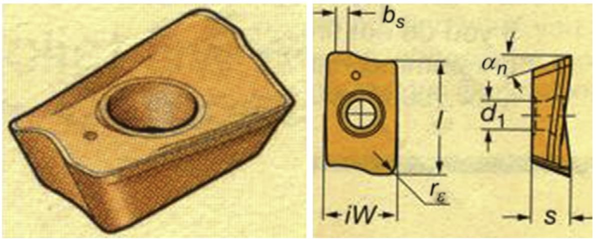

Figure 21 Insert shape and geometry. Reproduced from Main Catalogue, Sandvik Coromat, 2006.

Table 1 Insert geometry values

L	iW	d_1	s	b_S	r_ε	$\alpha_n 0$
11	6.8	2.8	3.59	1.2	0.8	21

Reproduced from Main Catalogue, Sandvik Coromat, 2006.

11.13.6.5.2 Workpiece Materials

Results of improvement in the machinability of two different work materials due to the application of induction heat-assisted machining are presented in this section. The materials are stainless steel AISI 304 and titanium alloy Ti–6Al–4V. The composition of stainless steel AISI 304 is: 0.08 C, 19 Cr, 9 Ni, and 2.0 Mn. The other material, Ti–6Al–4V, has $\alpha + \beta$ phases, and its composition is: 5.5–6.76 Al, 3.5–4.5 V, balance Ti.

11.13.6.5.3 Temperature Control for Preheating Experiments

In the induction heating system used during experiments, there was no online measurement of surface temperature during the machining process. In order to control the surface temperature, it was imperative to set the relationship of current input with temperature for different feed rates (traveling speed of the table). Preliminary experiments were performed to establish such a relationship. Figure 22 presents the experimental setup for determining the current–temperature–feed relationship.

The distance between the coil and workpiece was kept constant at 5 mm and was also maintained throughout all the experimental work. The sensing rod of a thermocouple was attached to the workpiece surface. The input current was set to

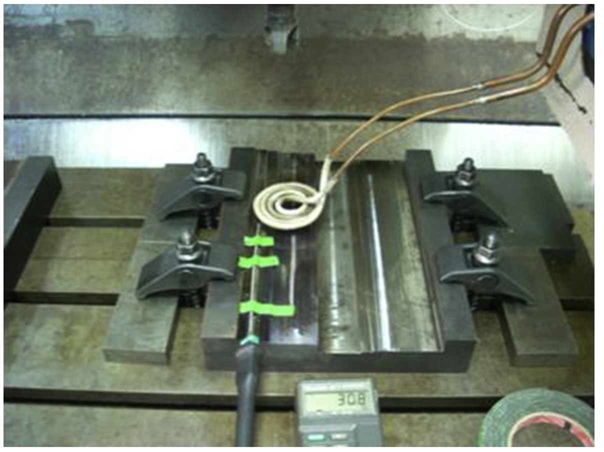

Figure 22 Experimental setup for determining the current–temperature–feed relationships. Reproduced from Turnad, L. G. Improvement of Machinability of Titanium Alloy Ti-6Al-4V through Workpiece Preheating. Ph.D. Thesis, Manufacturing and Materials Engineering Department, IIUM, Malaysia, 2009.

a particular value to produce a desired level of heating temperature on the workpiece surface. The workpiece was then passed with a specific feed rate, so that the sensing rod of thermocouple remained just below the coil. The surface temperature reading was taken, when the coil just passed the sensing rod of the thermocouple. The same trial was repeated two to three times for every experiment, and the average temperature was considered. Thus, for a particular current and feed value, the surface temperature was determined. The results of temperature control experiments for the feed are developed in heat-assisted machining. By using the regression method, characteristic equations of current as a function of temperature were developed at the 95% confidence interval. Those equations were then utilized to set the current value for a particular heating temperature. The input currents were set to reach the desired level of surface temperature during the preheated machining experiment.

11.13.7 Benefits of Induction Heat-Assisted End Milling of Stainless Steel AISI 304

These experiments were conducted using an induction heating system of relatively low-power capacity (25 KVA) for machining applications on work materials requiring low heating temperature. As discussed in the previous section, the heating temperature was maintained within $\pm 25\,^{\circ}\mathrm{C}$ at various table feed rates.

The influence of heating on three main aspects of machining, namely, chatter, surface roughness, and tool wear, were considered for two different cutting speeds (90 m min^{-1} and 150 m min^{-1}) at a constant depth of cut of 2 mm and two feed values of 0.1 mm per tooth and 0.2 mm per tooth. Sample data for two conditions with the higher values of feed and depth of cut (90 m min^{-1} and 150 m min^{-1}, and $D_C = 2$ mm and $Z_t = 0.2$ mm per tooth) are presented below.

11.13.7.1 Benefits in Terms of Chatter Suppression in the Frequency Range from 0 to 10 000 Hz

11.13.7.1.1 At Cutting Condition ($V_C = 90$ m s^{-1}, $D_C = 2$ mm, and $Z_t = 0.2$ mm per tooth)

Figure 23(a) and 23(b) shows the acceleration plots for the amplitudes when machining at room temperature and under heat-assisted machining conditions, respectively, in the frequency range of 0–5000, and Figure 24 summarizes the reduction in magnitude of the acceleration amplitudes for this condition.

The experiments found that an almost free vibration free-state was obtained since a reduction up to 98% was observed in the entire frequency range.

11.13.7.1.2 Benefits of Cutting Condition ($V_C = 150$ m s^{-1}, $D_C = 2$ mm, and $Z_t = 0.2$ mm per tooth)

Figures 25(a) and 25(b) shows the acceleration plots for the amplitudes when machining at room temperature and under heat-assisted machining conditions, respectively, in the frequency range of 0–5000, and Figure 26 compares the maximum acceleration amplitude peaks at different frequency intervals in this range under room temperature and heat-assisted machining of stainless steel at $275\,^{\circ}\mathrm{C}$.

Based on the results of these the experiments, almost free vibration free state was obtained since a reduction up to 98% was observed in the entire frequency range. Vibration results obtained under room temperature and heat-assisted machining in all the frequency ranges in the entire range of investigated parameters are shown in Table 2. As can be seen, the chatter amplitude in these cases is reduced up to almost 10 times.

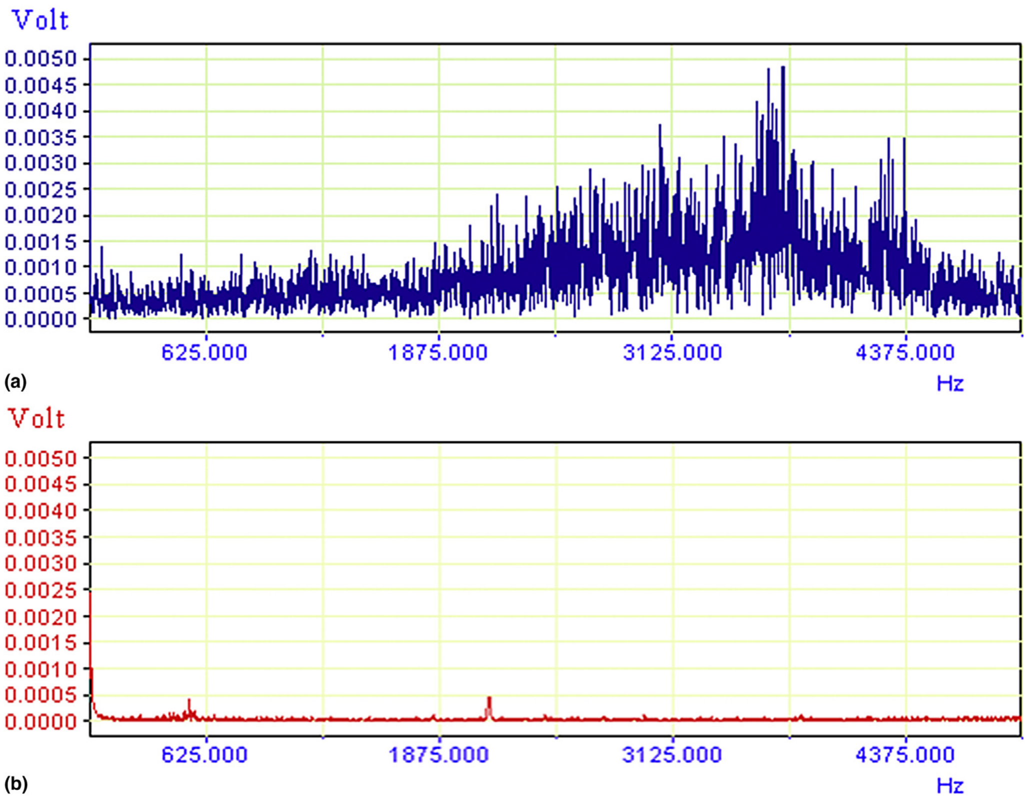

Figure 23 FFT plot for acceleration amplitudes under: (a) Room temperature condition; (b) Heat-assisted condition at 300 °C. * Conversion factor 1×10^{-3} V = 9.80665 m s^{-2}. Reproduced from Amin, A. K. M. N.; Abdelgadir, M. The Effect of Preheating of Work Material on Improved Machinability of Materials. In *Proceedings of the International Conference AIMTDR*, Ranchi, India, 2002.

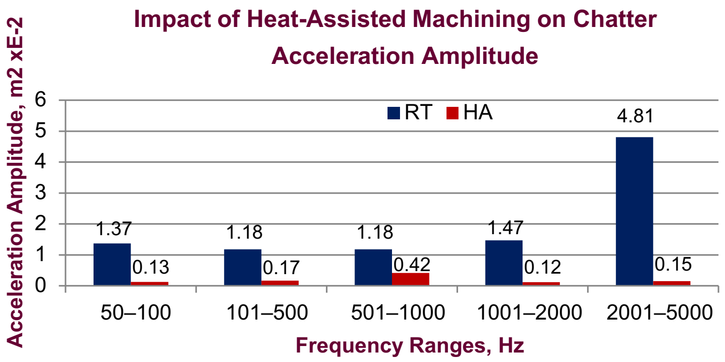

Figure 24 Comparison of maximum acceleration amplitude peaks at different frequency intervals in the range 0–5000 Hz under room temperature and heat-assisted machining of stainless steel at 300 °C.

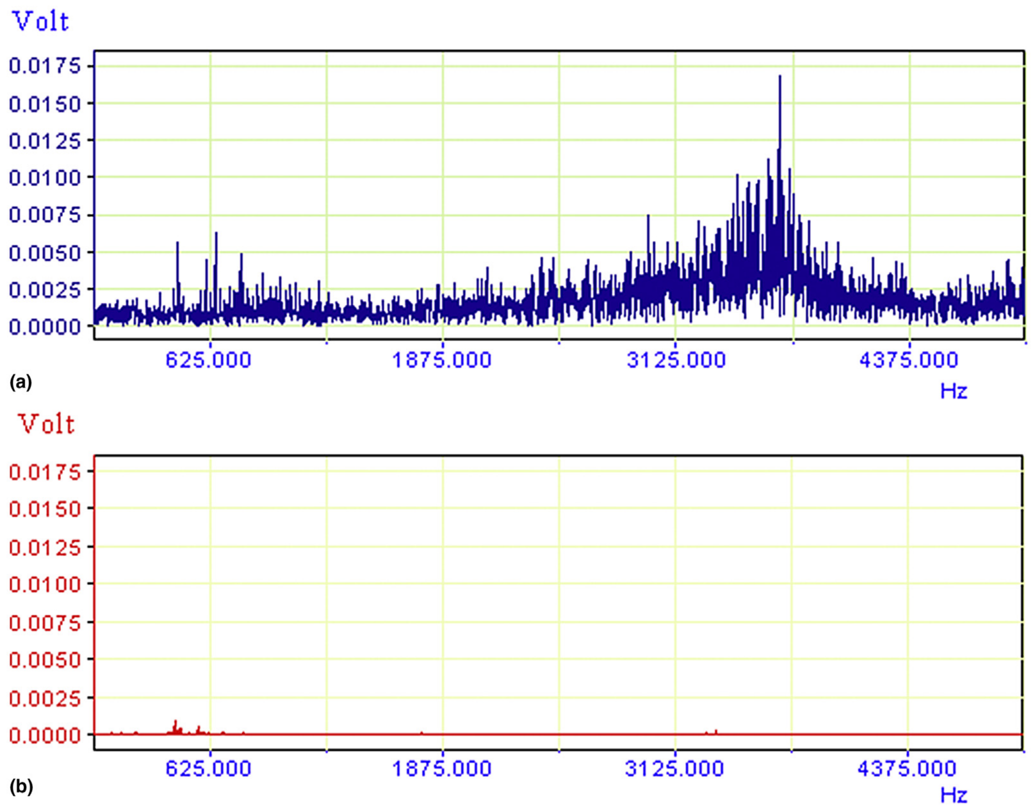

Figure 25 FFT plot for acceleration amplitudes under: (a) Room temperature condition; (b) Under heat-assisted condition at 265 °C. * Conversion factor 1×10^{-3} V = 9.80665 m s^{-2}. Reproduced from Amin, A. K. M. N.; Abdelgadir, M. The Effect of Preheating of Work Material on Improved Machinability of Materials. In *Proceedings of the International Conference AIMTDR*, Ranchi, India, 2002.

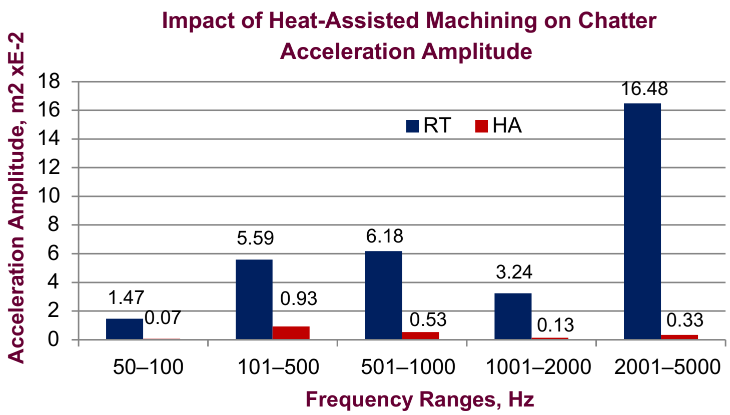

Figure 26 Comparison of maximum acceleration amplitude peaks at different frequency intervals in the range 0–5000 Hz under room temperature and heat-assisted machining of stainless steel at 265 °C.

Table 2 Vibration results obtained under room temperature and heat-assisted machining in all the frequency ranges in the entire range of investigated parameters in end milling of stainless steel

Cutting speed m s^{-1}	*Feed per tooth*	*Depth of cut (mm)*	*Temp. (°C)*		*Frequency range*				
					50–100	*100–500*	*500–1000*	*1000–2000*	*2000–5000*
90	0.1	1	R.T.	Frequency	0.03923	0.17652	0.08826	0.10787	0.20594
90			369.1	Amplitudes (m s^{-2})	0.00883	0.01961	0.02059	0.01765	0.05492
90		2	R.T.		0.03923	0.15691	0.07845	0.12749	0.29420
90			369.1		0.00588	0.02059	0.01275	0.01275	0.07747
90	0.2	1	R.T.		0.05884	0.22555	0.25497	0.07845	0.19613
90			300.6		0.00785	0.02844	0.00883	0.00883	0.01177
90		2	R.T.		0.13729	0.11768	0.11768	0.14710	0.48053
90			300.6		0.01275	0.01667	0.04217	0.01177	0.04511
120		1	R.T.		0.01275	0.01667	0.04217	0.01177	0.04511
120			325.6		0.00686	0.04805	0.01765	0.01079	0.04511
120	0.1	2	R.T.		0.03923	0.16671	0.08826	0.10787	0.14710
120			325.6		0.00686	0.08041	0.02157	0.00883	0.01667
120	0.2	1	R.T.		0.05884	0.21575	0.11768	0.10787	0.60801
120			290.6		0.00588	0.01275	0.01569	0.00588	0.00588
120		2	R.T.		0.11768	0.12749	0.19613	0.22555	0.86299
120			290.6		0.00588	0.06963	0.02550	0.01667	0.02648
150	0.1	1	R.T.		0.09807	0.08826	0.15691	0.12749	1.12776
150			309.3		0.00686	0.04707	0.03334	0.00981	0.01667
150		2	R.T.		0.04903	0.12749	0.08826	0.10787	0.61782
150			309.3		0.01471	0.04609	0.03236	0.05884	0.03923
150		1	R.T.		0.09807	0.57859	0.30401	0.42169	0.59821
150			274.5		0.00686	0.00981	0.02059	0.00785	0.01569
150	0.2	2	R.T.		0.14710	0.55898	0.61782	0.32362	1.64752
150			274.5		0.00686	0.09316	0.05296	0.01275	0.03334

Reproduced from Amin, A. K. M. N.; Abdelgadir, M. The Effect of Preheating of Work Material on Improved Machinability of Materials. In *Proceedings of the International Conference AIMTDR*, Ranchi, India, 2002.

11.13.7.2 Benefits in Terms of Surface Roughness Reduction

11.13.7.2.1 Benefits at Cutting Condition: $V_C = 90\,m\,s^{-1}$, $D_C = 2\,mm$, and $Z_t = 0.2\,mm$ per tooth and case IV ($V_C = 150\,m\,s^{-1}$, $D_C = 2\,mm$, and $Z_t = 0.2\,mm$ per tooth)

Table 3 summarizes the values of the R_a, R_γ, and R_z for both machining conditions. As is evident from Table xx, surface roughness – R_a, R_γ, and R_z are lowered by 28%, 23%, and 21%, respectively, in heat-assisted machining compared to room temperature conventional machining at 90 m min^{-1} at the given feed and depth of cut. The reductions in the R_a, R_γ, and R_z are by 32%, 48%, and 58%, respectively, at 90 m min^{-1} at the given feed and depth of cut due to the introduction of heat-assisted machining.

The surface roughness results obtained under room temperature and heat-assisted machining in the entire range of investigated cutting parameters are shown in Table 4. It can be observed that the surface roughness values of R_a, R_γ, and R_z are reduced substantially in all the cases.

11.13.7.3 Benefits in Terms of Tool Wear Reduction

Figures 27(a) and 27(b) shows the flank wear after room temperature and heat-assisted machining, respectively, at 90 m min^{-1}, and Figures 28(a) and 28(b) shows the flank wear after room temperature and heat-assisted machining, respectively, at 150 m min^{-1}. It is clear that there is substantial reduction in flank wear due to the introduction of heat-assisted machining at these two cutting speeds at the given feed and depth of cut.

Table 3 Comparison of R_a, R_y, and R_z values for the two machining conditions at 90 m min^{-1} and 150 m min^{-1}

Property measured	*Normal machining at V = 90 m min^{-1}*	*Heat-assisted machining at V = 90 m min^{-1}*	*(%) reduction at V = 90 m min^{-1}*	*Normal machining at V = 150 m min^{-1}*	*Heat-assisted machining at V = 150 m min^{-1}*	*(%) reduction at V = 150 m min^{-1}*
R_a (μm)	1.84	1.32	28	1.74	1.19	32
R_y (μm)	7.5	5.8	23	9.4	4.9	48
R_z (μm)	6.3	5.0	21	9.2	3.9	58

Reproduced from Amin, A. K. M. N.; Abdelgadir, M. The Effect of Preheating of Work Material on Improved Machinability of Materials. In *Proceedings of the International Conference AIMTDR*, Ranchi, India, 2002.

Table 4 Surface roughness results obtained under room temperature and heat-assisted machining in the entire range of investigated cutting parameters in the end milling of stainless steel

							Percent reduction		
Cutting speed (m min^{-1})	*Feed per tooth (mm)*	*Depth of cut (mm)*	*Temp. (mm)*	R_a	R_y	R_z	R_a	R_y	R_z
90	0.1	1	R.T.	0.68	2.70	2.50	42.65	14.81	24.00
			369.1	0.39	2.30	1.90			
		2	R.T.	0.89	4.40	3.50	11.24	18.18	17.14
			369.1	0.79	3.60	2.90			
	0.2	1	R.T.	1.35	6.80	6.20	17.04	23.53	17.74
			300.6	1.12	5.20	5.10			
		2	R.T.	1.84	7.50	6.30	28.26	22.67	20.63
			300.6	1.32	5.80	5.00			
120	0.1	1	R.T.	0.43	2.50	2.00	25.58	24.00	25.00
			325.6	0.32	1.90	1.50			
		2	R.T.	0.88	3.60	3.00	26.14	5.88	6.67
			325.6	0.65	3.40	2.80			
	0.2	1	R.T.	1.12	5.00	4.20	16.96	18.00	9.52
			290.6	0.93	4.10	3.80			
		2	R.T.	1.72	9.50	8.90	22.67	38.95	46.07
			290.6	1.33	5.80	4.80			
150	0.1	1	R.T.	1.10	5.00	3.10	39.09	24.00	22.58
			309.3	0.67	3.80	2.40			
		2	R.T.	0.96	3.60	3.00	18.75	5.56	6.67
			309.3	0.78	3.40	2.80			
	0.2	1	R.T.	1.56	5.60	4.90	23.72	25.00	20.41
			274.5	1.19	4.20	3.90			
		2	R.T.	1.74	9.40	9.20	31.61	47.87	57.61
			274.5	1.19	4.90	3.90			

Reproduced from Amin, A. K. M. N.; Abdelgadir, M. The Effect of Preheating of Work Material on Improved Machinability of Materials. In *Proceedings of the International Conference AIMTDR*, Ranchi, India, 2002.

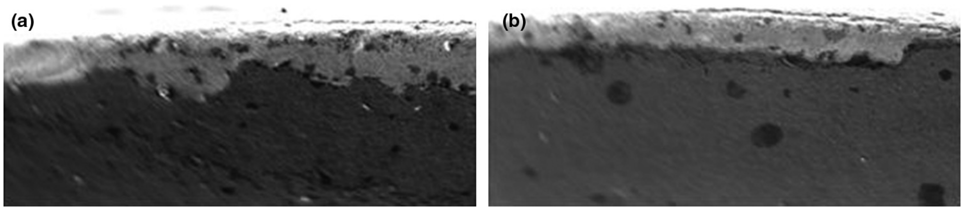

Figure 27 Flank wear, stainless steel for machining: (a) At room temperature; (b) Under heat assistance at 275 °C at 90 m min^{-1}, depth of cut 2 mm, and feed 0.2 mm per tooth. Reproduced from Amin, A. K. M. N.; Abdelgadir, M. The Effect of Preheating of Work Material on Improved Machinability of Materials. In *Proceedings of the International Conference AIMTDR*, Ranchi, India, 2002.

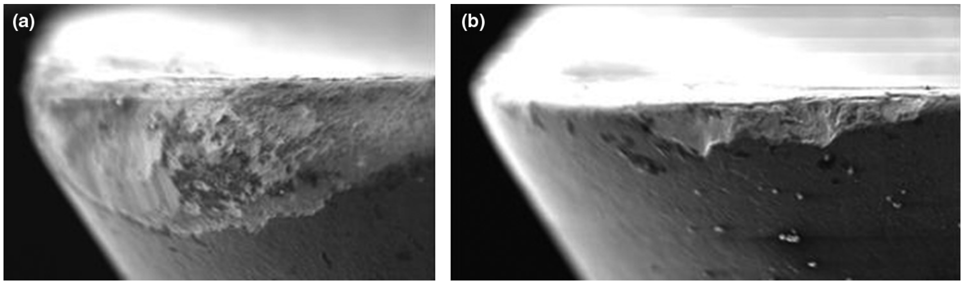

Figure 28 Flank wear, stainless steel for machining: (a) At room temperature; (b) Under heat assistance at 265 °C at 150 m min^{-1}, depth of cut 2 mm, and feed 0.2 mm per tooth. Reproduced from Amin, A. K. M. N.; Abdelgadir, M. The Effect of Preheating of Work Material on Improved Machinability of Materials. In *Proceedings of the International Conference AIMTDR*, Ranchi, India, 2002.

11.13.8 Benefits of Induction Heat-Assisted End Milling of Titanium Alloy – Ti–6Al–4V

This chapter presents results obtained through various experiments and investigations to assess the effect of heat-assisted machining on the improvement of machinability in the end milling of Ti–6Al–4V alloy with uncoated WC–Co inserts, followed by relevant discussions. These experiments were conducted using an induction heating system of higher power capacity (35 kW) since titanium requires higher heating temperature compared to carbon and stainless steel. The major machinability criteria that have been critically analyzed as functions of primary machining variables as well as preheating temperatures are as follows:

- Tool life and tool wear morphology
- Cutting forces
- Vibration/chatter
- Surface roughness and surface integrity
- Chips morphology

The influence of heating on different aspects of machinability, namely, cutting force, chatter, surface roughness, tool wear, metal removal rate, chip formation, and surface integrity of the machined part, was considered. The design of experiments and the cutting conditions for this part are shown in Section 11.13.7.

11.13.8.1 Effect on Vibration/Chatter

Vibration/chatter in machining is an undesirable but unavoidable phenomenon. The term is defined as the self-excited violent relative dynamic motion between the cutting tool and workpiece. In the current study, Fast Fourier Transformation (FFT) analysis of the time-domain vibration signals, captured by the accelerometer mounted on the spindle, was conducted using the DASYLab 5.5 software. FFT for four different conditions, at room temperature, and for three different temperatures of heat application are presented for comparison in Figures 29(a–d). The machining parameters used in these experiments were cutting speed = 70 m min^{-1}, feed = 0.088 mm per tooth, axial depth of cut = 1 mm. These diagrams show that heat-assisted machining has a great influence on vibration and chatter in end milling of titanium alloy Ti–6Al–4V. As can be observed from the figures, there are four main peaks of amplitude in the range of 0–12 500 Hz. These peaks are eventually used to analyze the effects of preheating on the amplitude of chatter acceleration.

The maximum acceleration amplitudes for room temperature and heat-assisted machining at different heating temperatures are presented in Table 5 along with the percentage of reductions at the respective heating temperatures compared to room temperature amplitudes. Reduction of acceleration of amplitude was found to range from 25 to 50%, 42.9 to 66.7%, and 64.3 to 88.2% at 315, 450, and 650 °C, respectively.

The reductions of the peak values are systematically calculated, and the effects of heating temperature on the amplitudes are plotted as bar charts in Figure 30. It is observed clearly that the amplitude of all four peaks in the frequency range from 0 to 12 000 Hz experience drastic reduction due to heat-assisted machining. The reduction is found to increase with the heating temperature, with the highest value at the highest heating temperature of 650 °C.

The results therefore suggest that heat-assisted machining can be employed successfully to suppress vibration/chatter in the machining of titanium alloy Ti–6Al–4V. Reduction of chatter during cutting due to heat-assisted machining decreases the dynamic loading on the tool tips and plays a favorable role in reducing tool wear and improving surface finish.

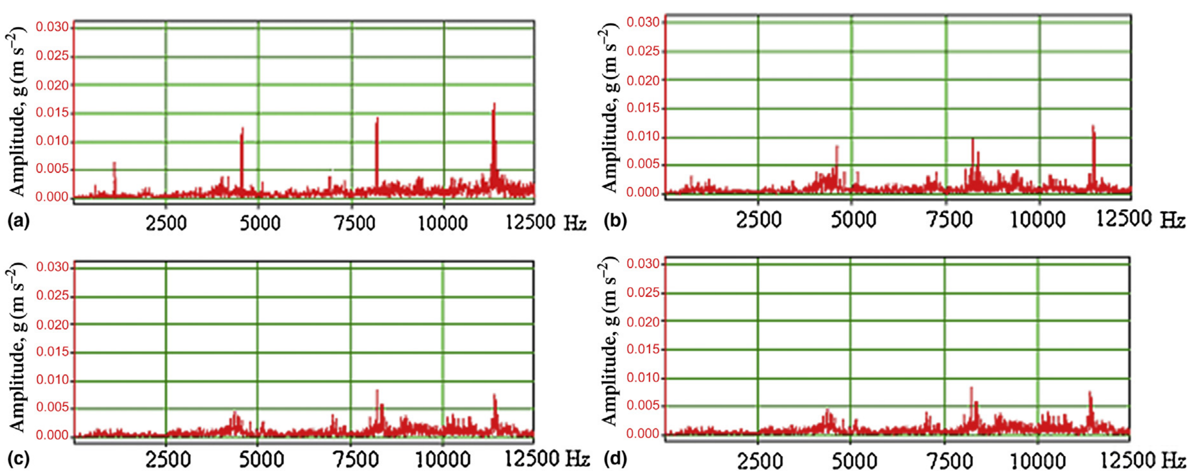

Figure 29 FFT output of end milling with uncoated WC–Co: (a) At room temperature; (b) Preheating at 315 °C; (c) Preheating at 450 °C; (d) Preheating at 650 °C (cutting speed = 70 m min^{-1}, axial DOC = 1 mm, feed = 0.088 mm per tooth). Reproduced from Turnad, L. G. Improvement of Machinability of Titanium Alloy Ti-6Al-4V through Workpiece Preheating. Ph.D. Thesis, Manufacturing and Materials Engineering Department, IIUM, Malaysia, 2009.

Table 5 Acceleration amplitudes of vibration and the percentage of reduction (inserts: uncoated WC–Co)

	Maximum acceleration amplitude ($m\,s^{-2}$)				*Amplitude reductions (%)*		
Frequency range (Hz)	*R.T.*	*315 °C*	*450 °C*	*650 °C*	*315 °C*	*450 °C*	*650 °C*
0–2500	0.006	0.003	0.002	0.001	50	66.7	83.3
2500–5000	0.012	0.009	0.005	0.003	25.2	58.3	75
7500–10 000	0.014	0.010	0.008	0.005	28.6	42.9	64.3
10 000–12 500	0.017	0.012	0.007	0.002	29.4	58.8	88.2

Reproduced from Turnad, L. G. Improvement of Machinability of Titanium Alloy Ti-6Al-4V through Workpiece Preheating. Ph.D. Thesis, Manufacturing and Materials Engineering Department, IIUM, Malaysia, 2009.

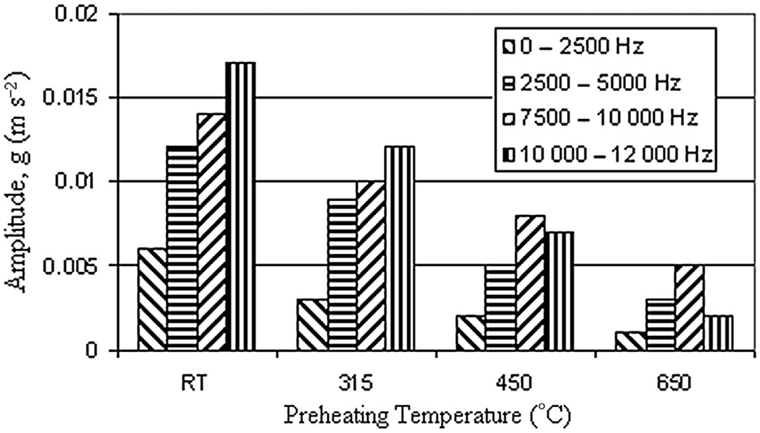

Figure 30 The effect of heating temperature on acceleration amplitude of vibration (cutting speed = 70 m min^{-1}, axial DOC = 1 mm, feed = 0.088 mm per tooth, insert: uncoated WC–Co). Reproduced from Turnad, L. G. Improvement of Machinability of Titanium Alloy Ti-6Al-4V through Workpiece Preheating. Ph.D. Thesis, Manufacturing and Materials Engineering Department, IIUM, Malaysia, 2009.

11.13.8.2 Effect on Cutting Force

This section presents a comparison of cutting force under these two conditions and discusses in detail the effects of heating temperature, cutting speed, as well as feed on cutting force. The resultant cutting forces recorded from the experiments were used for comparison.

The effects of heating temperature and cutting speed on the resultant cutting force are presented in Figure 31. The figure affirms that an increase in heating temperature as well as cutting speed leads to reduction of the resultant cutting force. For instance, the resultant cutting force is found to be reduced by 44.5 and 40.6% at 30.6 and 160 m min^{-1}, respectively, due to heating at only 450 °C (the optimum heating temperature being 650 °C). On the other hand, an increase in cutting speed from 30.6 to 160 m min^{-1} reduces the resultant cutting force by 36.8 and 32.5% for room temperature and heat-assisted machining respectively.

The effect of heat-assisted machining conducted using three different feed values was investigated. Figure 32 presents the results of this investigation. Cutting force is also found to drastically rise with the increase of feed. However, the reduction in cutting force due to heat-assisted machining is clearly indicated in the figure for all three feed values applied in the experiments.

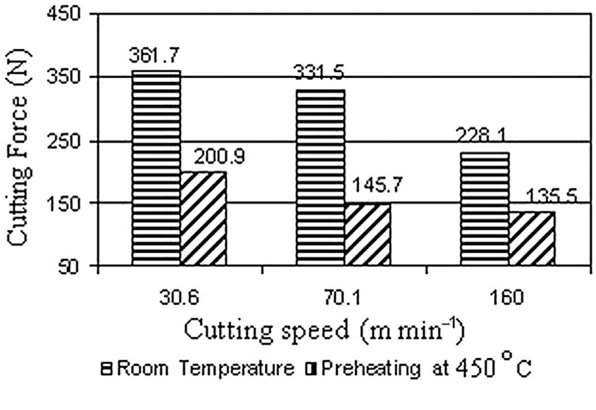

Figure 31 Combined effects of cutting speed and heat assistance (at 450 °C) on the resultant cutting force (insert: uncoated WC–Co). (Feed = 0.088 mm per tooth and axial depth of cut = 1 mm). Reproduced from Turnad, L. G. Improvement of Machinability of Titanium Alloy Ti-6Al-4V through Workpiece Preheating. Ph.D. Thesis, Manufacturing and Materials Engineering Department, IIUM, Malaysia, 2009.

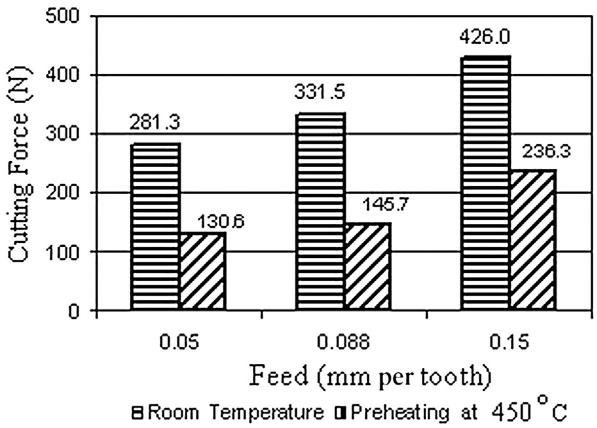

Figure 32 Effects of feed and heat assistance (at 450 °C) on the resultant cutting force (insert: uncoated WC–Co). (Cutting speed = 70.1 m min^{-1} and axial depth of cut = 1 mm). Reproduced from Turnad, L. G. Improvement of Machinability of Titanium Alloy Ti-6Al-4V through Workpiece Preheating. Ph.D. Thesis, Manufacturing and Materials Engineering Department, IIUM, Malaysia, 2009.

As shown in Figure 32, the cutting force increases by 51.4 and 81.1% when feed is increased from 0.05 to 0.15 mm per tooth for room temperature and heat-assisted conditions, respectively. The reduction in the resultant force by 53.6 and 44.5% at the feed of 0.05 and 0.088 mm per tooth, respectively, was achieved by heating the workpiece at only 450 °C is applied. This is attributable to the drop in the yield strength of the workpiece material at the elevated temperature during the heat-assisted end milling, which eventually reduces the normal and the shear stresses acting on the tool and thus contributes to lower the cutting forces.

The effect of heating temperature on the resultant force was investigated for a given set of cutting parameters: Cutting speed = 70 m min^{-1}, axial DOC = 1 mm, feed = 0.088 mm per tooth. Figure 33 illustrates the effect of heating temperature on cutting force. The resultant cutting force decreases sharply from 331.5 N at room temperature to 177.6 N at 315 °C. With further increase in heating temperature, the reduction is more gradual. The resultant force is reduced to only 134 N at 650 °C.

11.13.8.3 Effect on Tool Wear and Tool Wear Morphology

Figures 34 and 35 compare tool life and volume of metal removal (VMR) per tool life, respectively, in the cutting speed range from 30 m min^{-1} up to 160 m min^{-1} for the given insert (WC–Co). Tool life and volume of metal removal per tool life at heat-assisted machining are much higher compared to room temperature machining, though these two parameters are found to decline with the increase in cutting speed, especially beyond 70 m min^{-1}. Tool life and VMR are insignificant at the highest cutting speed of 160 m min^{-1}. The maximum benefit of heat-assisted machining can be derived at the cutting speed of 70 m min^{-1}, since the VMR is the same as at the lower speed of 30 m min^{-1} and application of this speed would ensure higher productivity. At this cutting speed, tool life is increased by 205.6% and VMR by 214.3% compared to the corresponding room temperature condition.

The effects of heating temperature on tool life and tool life improvement at constant cutting speed of 70 m min^{-1} are presented in Figure 36. Interestingly, the heating of work material substantially improves tool life, and as a result, enhances the VMR. However, at lower heating temperature (e.g., 315 °C), there is insignificant improvement in tool life. But as the temperature was

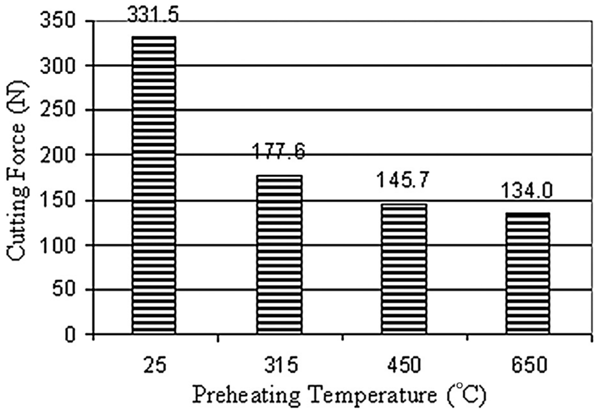

Figure 33 Effect of heating temperature on the resultant of cutting force (cutting speed = 70 m min^{-1}, axial DOC = 1 mm, feed = 0.088 mm per tooth, insert: uncoated WC–Co). Reproduced from Turnad, L. G. Improvement of Machinability of Titanium Alloy Ti-6Al-4V through Workpiece Preheating. Ph.D. Thesis, Manufacturing and Materials Engineering Department, IIUM, Malaysia, 2009.

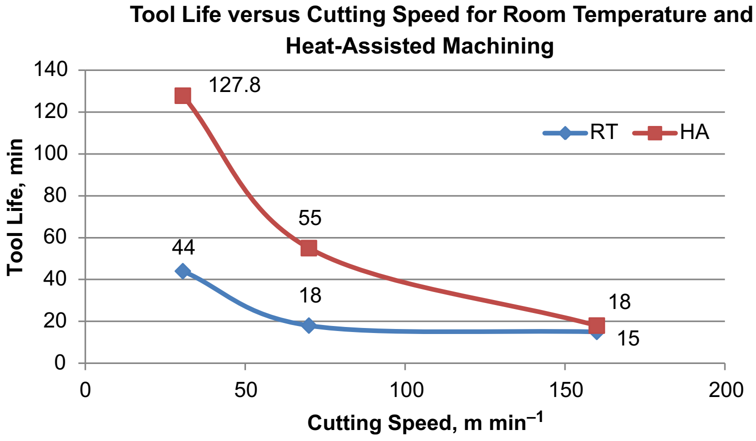

Figure 34 Comparison of tool life under room temperature and heat-assisted machining (cutting speed = 70 m min^{-1}, axial DOC = 1 mm, feed = 0.088 mm per tooth, insert: uncoated WC–Co).

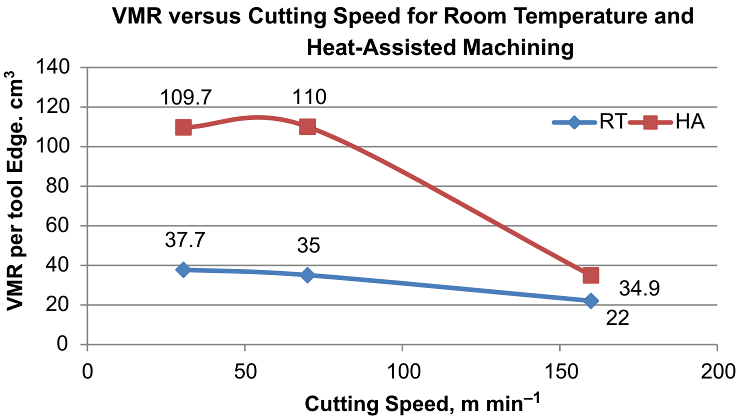

Figure 35 Comparison of volume of metal removal per tool life under room temperature and heat-assisted machining (cutting speed = 70 m min^{-1}, axial DOC = 1 mm, feed = 0.088 mm per tooth, insert: uncoated WC–Co).

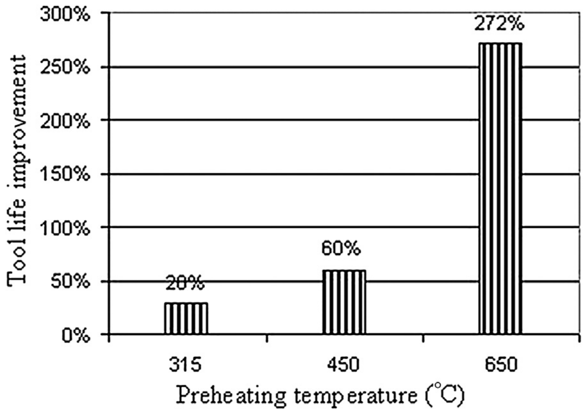

Figure 36 Effects of heating temperature on (a) Tool life; (b) Tool life improvement (cutting speed = 70 m min^{-1}, axial DOC = 1 mm, feed = 0.088 mm per tooth, insert: uncoated WC–Co). Reproduced from Turnad, L. G. Improvement of Machinability of Titanium Alloy Ti-6Al-4V through Workpiece Preheating. Ph.D. Thesis, Manufacturing and Materials Engineering Department, IIUM, Malaysia, 2009.

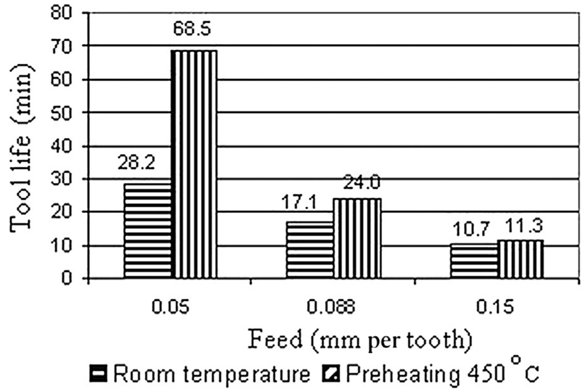

Figure 37 Effects of feed on tool life (cutting speed = 70 m min^{-1}, axial DOC = 1 mm, insert: uncoated WC–Co). Reproduced from Turnad, L. G. Improvement of Machinability of Titanium Alloy Ti-6Al-4V through Workpiece Preheating. Ph.D. Thesis, Manufacturing and Materials Engineering Department, IIUM, Malaysia, 2009.

increased, a significant improvement in tool life was achieved. This is related to the earlier results showing that heating of work material suppressed chatter/vibration and lowered the cutting force. With heating at 650 °C, tool life is increased by more than 270%. Hence 650 °C may be considered as the optimum heating temperature for the given work material (Ti–6Al–4V). The findings confirm that induction coil heat-assisted end milling is a prospective method in enhancing the tool life.

The effect of heat-assisted machining for three different feed values are illustrated in Figure 37. The benefit of heat-assisted machining conducted at 450 °C is maximum at the lowest feed of 0.05 m per tooth, and at the higher feed rate the effect is lower. Perhaps higher heating temperature of up to 650 °C is required to heat up the thicker undeformed chip thickness in order to derive the full benefit of heat-assisted machining.

11.13.8.4 Tool Wear Morphology

The scanning electron microscope (SEM) was used in the investigation of tool wear morphology. The effects of cutting speed, feed, axial depth of cut, and heating temperature on the tool wear profile were thoroughly investigated. The findings of these investigations are presented in this section.

Figure 38 compares the SEM pictures of worn tools after heat-assisted machining at different temperatures. Heat-assisted machining guarantees superior tool life in the end milling of Ti–6Al–4V, as previously exemplified in Section 8.3. This fact is also verified and substantiated by analyzing and comparing the tool wear for both room temperature and heat-assisted machining conditions. The experimental runs with the same cutting speed, feed, axial depth of cut but with different temperatures have been essentially selected for this purpose.

Figure 38 shows that flank wear is reduced to different degrees after heating to different temperatures compared to that under room temperature conditions. Nonuniform flank wear and attrition type wear are found to be more prevalent in room temperature, and heat-assisted machining applying low heating temperature of 315 °C and diffusion wear are the most prominent in other two cases of heat-assisted machining, with higher heating temperatures of 450 and 650 °C. One cause of this appreciable reduction of tool wear is related to the reduction of acceleration amplitude of vibration/chatter due to heat-assisted machining (*6*). Among other reasons for lower tool wear is the lower cutting force during heat-assisted machining and reduction of dynamic loads acting on the tool. Softer workpiece with reduced shear strength as a result of heating effectively helps reduce the stress acting on the tool, and it is responsible for reducing tool wear, leading to increased tool life. Heat-assisted machining reduces the strain hardening and flow stress of material, which also contribute to increased tool life.

Figures 39(a–d) shows the SEM views of chip-tool contact length for room temperature and heat-assisted machining. As seen in these figures, heating temperature markedly increases the chip-tool contact length. Figure 40 illustrates the effect of heating temperature on chip-tool contact length. It can be observed from Figure 40 that the contact length is increased from 185 μm at room temperature to 280 μm at 650 °C of preheating; that is, chip-tool contact length is increased by 51.4%.

Longer chip-tool contact length in heat-assisted machining is beneficial in two ways: first, it shifts the hot spot away from the cutting edge, and second, the normal stress acting on the tool becomes lower (*4*). Heating also results in lower frictional forces acting on the rake face of the tool because of the lower shear strength of the flow zone materials owing to the higher temperature of the zone. As a result, dynamic loads that act on the tool are substantially lower for heat-assisted machining compared to room temperature machining. All of these aspects add to the benefits of heat-assisted machining.

11.13.8.5 Surface Roughness and Surface Integrity

This section presents a comparison of surface roughness obtained under room temperature and heat-assisted machining conditions. In these investigations, the heating temperature was only varied keeping the machining conditions same for both machining

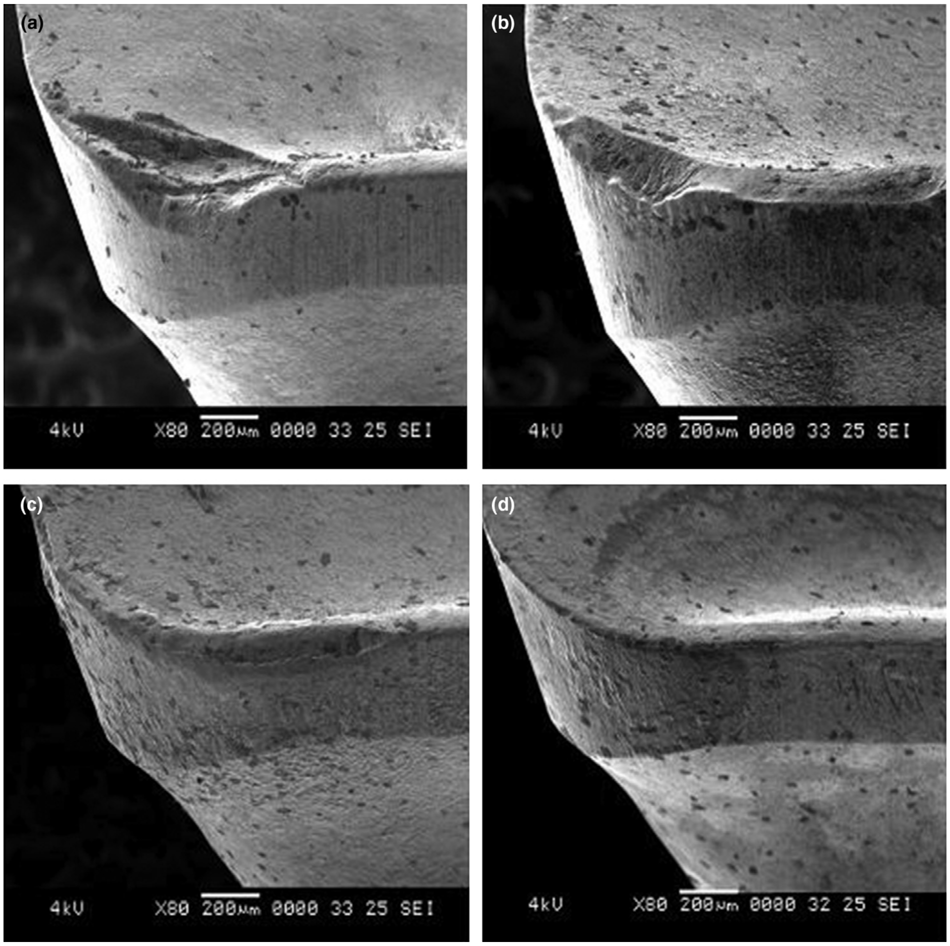

Figure 38 SEM views of worn tools at: (a) Room temperature (tool life: 17.1 min); (b) Heating at 315 °C (tool life: 19.2 min); (c) Heating at 450 °C (tool life: 23.5 min); (d) Heating at 650 °C (tool life: 55.7 min) (cutting speed = 70 m min^{-1}, axial DOC = 1 mm, feed = 0.088 mm per tooth, insert: uncoated WC–Co). Reproduced from Turnad, L. G. Improvement of Machinability of Titanium Alloy Ti-6Al-4V through Workpiece Preheating. Ph.D. Thesis, Manufacturing and Materials Engineering Department, IIUM, Malaysia, 2009.

methods. The surface integrity and subsurface alternation have also been thoroughly investigated by employing SEM and Vickers microhardness testing. Microhardness was measured to observe the distributions of the hardness beneath the machined surface and to determine the effect of heating on subsurface hardness and microstructure. The changes in microstructure were investigated using a SEM. The effects of heating on the subsurface alternations are discussed in this section. Prior to investigating surface integrity, samples were prepared by cutting the work specimen perpendicular to machined surfaces using electro discharge wire cutting. The samples were then mounted using hot mounting, and grounded using silicon carbide abrasive papers, followed by polishing with alumina solutions, and finally etched with 10% HF, 5% HNO_3, 85% H_2O solutions. Microhardness was measured along the depth (perpendicular to the machined surface), at an interval of 0.01 mm from the top surface up and continued up to a depth of 0.5 mm.

The dependence of surface roughness on heating temperature is shown in Figure 41. As the figure illustrates, surface roughness is sharply reduced from the room temperature value of 0.25–0.19 μm when hot machined at 315 °C. Surface roughness value is found to slightly increase as the heating temperature is further increased up to 650 °C. Suppressed vibration/chatter amplitude during heat-assisted machining and higher heating temperature at the chip-tool interface facilitating easier chip flow are the main factors contributing to reducing surface roughness.

Increasing trends toward surface roughness values at higher heating temperature may be attributable to the higher chemical reactivity of the work material, which encourages welding between chips and tools to form a pile-up of material similar to built-up edge (BUE), which is more prominent in the case of preheated machining, as shown in Figures 42(a–d). Similar to room temperature machining, the presence of BUE can be observed in most of the cutting conditions under preheated machining. This is attributed to the high chemical reactivity between the chip and cutting tool. At a cutting speed of 70 m min^{-1} (Figures 42(a) and 42(b)), the BUE is very stable, but at 126 and 160 m min^{-1} it is unstable and scattered (Figures 42(c) and 42(d)). As the preheating temperature is increased, the chemical reactivity drastically increases. The BUE is developed on the rake face and in the flank face, similar to cutting at room temperature. Essentially, the stable BUE developed helps to protect the tool from wear by acting as a shield on the tool tip. Unstable BUE, on the other hand, causes a higher rate of wear and adversely affects the surface finish.

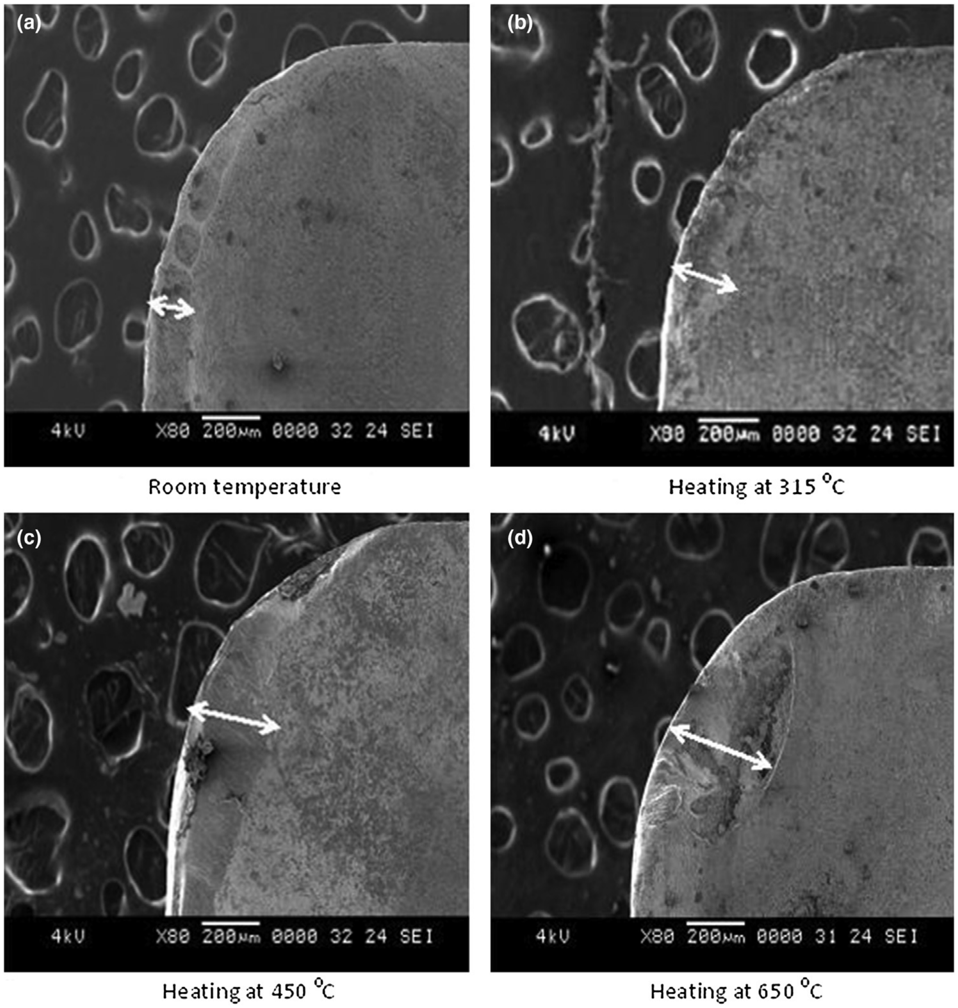

Figure 39 SEM views of chip-tool contact length (cutting speed = 70 m min^{-1}, axial DOC = 1 mm, feed = 0.088 mm per tooth, insert: uncoated WC–Co). Reproduced from Turnad, L. G. Improvement of Machinability of Titanium Alloy Ti-6Al-4V through Workpiece Preheating. Ph.D. Thesis, Manufacturing and Materials Engineering Department, IIUM, Malaysia, 2009.

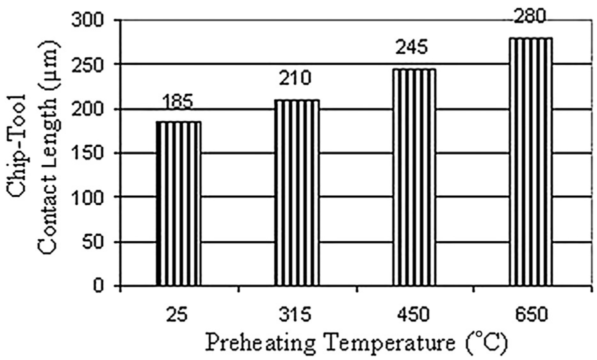

Figure 40 Chip-tool contact length versus preheating temperature (cutting speed = 70 m min^{-1}, axial DOC = 1 mm, feed = 0.088 mm per tooth, insert: uncoated WC–Co). Reproduced from Turnad, L. G. Improvement of Machinability of Titanium Alloy Ti-6Al-4V through Workpiece Preheating. Ph.D. Thesis, Manufacturing and Materials Engineering Department, IIUM, Malaysia, 2009.

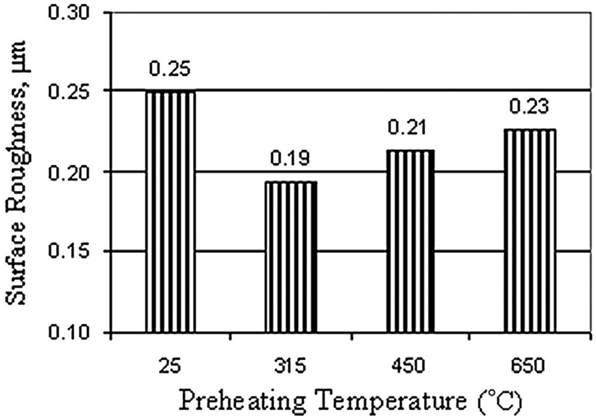

Figure 41 Effects of heating temperature on surface roughness (cutting speed = 70 m min^{-1}, axial DOC = 1 mm, f = 0.088 mm per tooth, insert: uncoated WC–Co). Reproduced from Turnad, L. G. Improvement of Machinability of Titanium Alloy Ti-6Al-4V through Workpiece Preheating. Ph.D. Thesis, Manufacturing and Materials Engineering Department, IIUM, Malaysia, 2009.

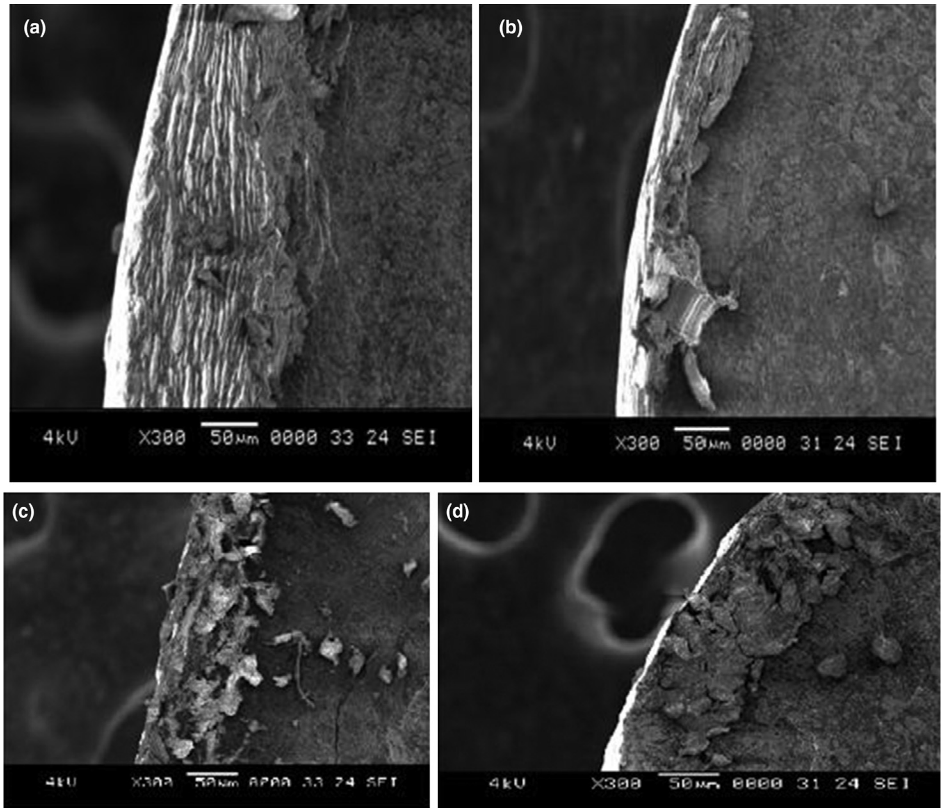

Figure 42 SEM views of built-up edge under preheated conditions: (a) $V = 70$, $f_z = 0.05$, $d = 1$, Temp = 315; (b) $V = 70$, $f_z = 0.088$, $d = 1$, Temp = 450; (c) $V = 126$, $f_z = 0.06$, $d = 1$, Temp = 580; (d) $V = 160$, $f_z = 0.088$, $d = 1$, Temp = 450 (insert: uncoated WC–Co). Reproduced from Turnad, L. G. Improvement of Machinability of Titanium Alloy Ti-6Al-4V through Workpiece Preheating. Ph.D. Thesis, Manufacturing and Materials Engineering Department, IIUM, Malaysia, 2009.

11.13.8.6 Surface Integrity and the Underlying Layer

11.13.8.6.1 Surface Integrity

The surface integrity of machined surfaces has been investigated by employing the SEM. The objective of the investigation is to identify the presence of defects, such as cracks, droplets of BUE, or chip fragments on machined surfaces, especially at higher heating temperature, to explore the causes of increased surface roughness when the heating temperature is increased beyond 315 °C, as discussed in the previous subsection. In Figures 43(a) and 43(b), the presence of some chip fragments and BUE on the surface for both room temperature and heat-assisted machining is clearly seen. High temperature generated during cutting of Ti–6Al–4V is

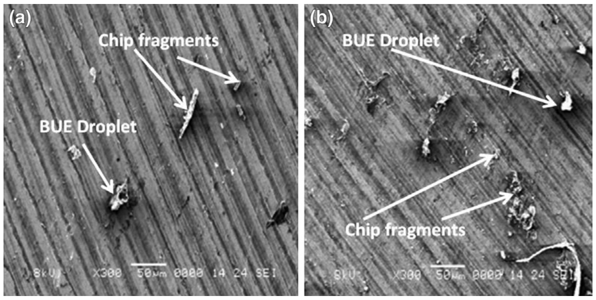

Figure 43 SEM views of machined surface in end milling at: (a) Room temperature; (b) Heating at 650 °C (cutting speed = 70 m min^{-1}, axial DOC = 1 mm, feed = 0.088 mm per tooth, insert: uncoated WC–Co). Reproduced from Turnad, L. G. Improvement of Machinability of Titanium Alloy Ti-6Al-4V through Workpiece Preheating. Ph.D. Thesis, Manufacturing and Materials Engineering Department, IIUM, Malaysia, 2009.

mainly responsible for the buildup of chip fragments on the machined surface, which finally depreciates the surface finish. Application of high-pressure air blowing directed to the machining zone during operation could eliminate the formation of these depositions and thereby improve the surface finish further.

11.13.8.6.2 The Underlying Layer

For this investigation the distribution of the microhardness below the surface layer was recorded under different cutting conditions. Apart from that, the microstructure of the layer below the surface was also investigated. Distributions of microhardness measured up to certain depths beneath the surface after end milling with uncoated WC–Co inserts under room temperature and two heating temperature are informatively presented in Figure 44. The measurements were taken at a length interval of 0.01 mm starting from the top surface up to a depth of 0.5 mm beneath the surface. According to the hardness, the surface layer is divided into three zones: the heat-affected zone (Zone I), the strain-hardened zone (Zone II), and the base material (Zone III).

Microhardness values in Zone I are relatively lower than those of the strain-hardening zone (Zone I) and the base materials (Zone III) as shown in Figure 44. It may be related to the fact that the heat that is generated during cutting leads to softening of a thin layer below the surface due to annealing. As the heating temperature increases, the driving force for annealing obviously increases, which results in lower microhardness. For instance, the distribution of microhardness after end milling at heating temperature of 650 °C is slightly lower compared to those under room temperature and heat-assisted machining at 315 °C, as shown in Figure 44. The figure also shows that Zone I reaches the range of up to ~0.15 mm below the surface. In the zone more than 0.15 mm from the surface, the effect of heating substantially decreases, which is inadequate as a driving force for annealing arrangement. Due to the plastic deformation, the microhardness in this zone (Zone II) is also relatively high and is then considered as a strain-hardening zone. Moreover, as the distance from the surface increases, the strain-hardening effect caused by shearing and plastic deformation gradually decreases, and as a result, the distribution hardness returns to the initial value (base metal). In the case of end milling with uncoated WC–Co inserts, the distance of the strain-hardening zone is found to be up to 0.4 mm beneath the surface.

Under room temperature machining, the heat generated during cutting has less effect on the microstructure alteration. No appreciable grain growth occurs in this condition, as presented in Figure 45(b) compared to the original microstructure (Figure 45(a)). When heat-assisted machining is applied at 650 °C, there is a slight grain growth as shown in Figure 45(c). In metallurgical terms, an increase in the size of grains decreases the hardness of the materials, as also observed at the beginning of this subsection.

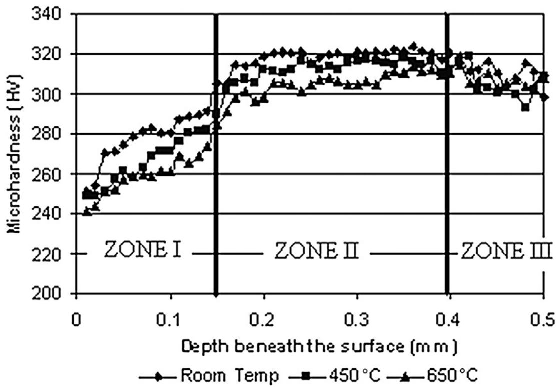

Figure 44 Microhardness value beneath the machined surface in end milling with uncoated WC–Co inserts (cutting speed = 70 m min^{-1}, axial DOC = 1 mm, feed = 0.088 mm per tooth). Reproduced from Turnad, L. G. Improvement of Machinability of Titanium Alloy Ti-6Al-4V through Workpiece Preheating. Ph.D. Thesis, Manufacturing and Materials Engineering Department, IIUM, Malaysia, 2009.

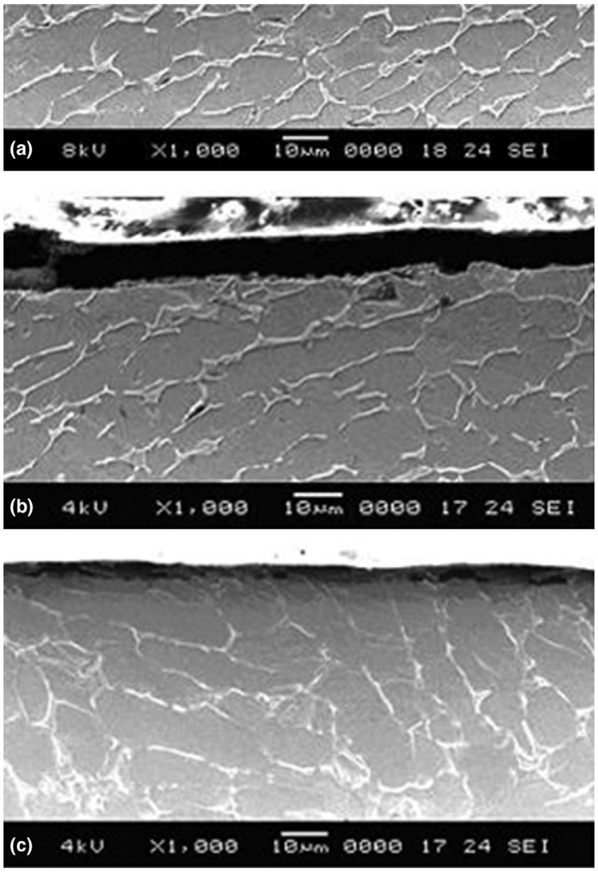

Figure 45 Microstructure alterations in end milling: (a) The base metal; (b) Room temperature; (c) Heating at 650 °C (Insert: uncoated WC–Co, cutting speed = 70 m min^{-1}, axial DOC = 1 mm, feed = 0.088 mm per tooth). Reproduced from Turnad, L. G. Improvement of Machinability of Titanium Alloy Ti-6Al-4V through Workpiece Preheating. Ph.D. Thesis, Manufacturing and Materials Engineering Department, IIUM, Malaysia, 2009.

11.13.8.7 Chips Morphology

Chips formed during room temperature and heat-assisted machining conditions were analyzed carefully in order to determine the effects of heating on the phenomenon such as chip serration, chip shrinkage coefficient, and chip forming frequency. Figures 46(a–d) presents the SEM views of the chips formed at different heating temperatures. The figures are arranged serially with increasing temperature. It can be observed from the SEM views of chips that there are chip serrations running across the whole width of the chips in all the investigated cases. These teeth are termed *primary serrated teeth*. There are also marks of grouping of several primary serrated elements at the upper free edge and in some cases at the lower tool nose-side edge of the chip. These larger coagulated elements are known as *secondary serrated teeth*. This section presents the effect of online heating temperature on the primary serration of chip.

Frequency of the chip serration was calculated using the parameters cutting speed, coefficient of chip shrinkage, magnification of the SEM micrograph, and numbers of serrated elements (number of serrated teeth). The chip shrinkage coefficient is shown in Figure 47 as a function of preheating (heating) temperature.

Figures 48(a–c) presents a cross-section of chips produced during end milling at a particular set of cutting parameters (cutting speed = 70 m min^{-1}, f_z = 0.088 mm per tooth, axial DOC = 1 mm, insert: uncoated WC–Co) conducted under three different cutting conditions: room temperature and at two heating temperatures (450 °C and 650 °C). Figure 46 shows that the chips become more stable with the increase in heating temperature. The chips are almost continuous, practically without serration at the heat-assisted temperature of 650 °C (Figure 46(c)). A lower peak-to-valley ratio of the chip was found during employing heating. The peak-to-valley ratio decreases with the increase in heating temperature and comes to almost 1 at the highest heating temperature of 650 °C.

Figure 49 shows the peak-to-valley ratio versus heating temperature for chips produced at the cutting speed of 70 m min^{-1}, feed = 0.088 mm per tooth, and axial DOC = 1 mm using uncoated WC–Co inserts *(44)*.

11.13.8.8 Discussion

The results of experiments presented in this section clearly show that heat-assisted machining appreciably increased the tool life and VMR. For instance, at a cutting speed of 30.6 m min^{-1}, 44 min of tool life, and 37.7 cm^3 of VMR were achieved in room temperature

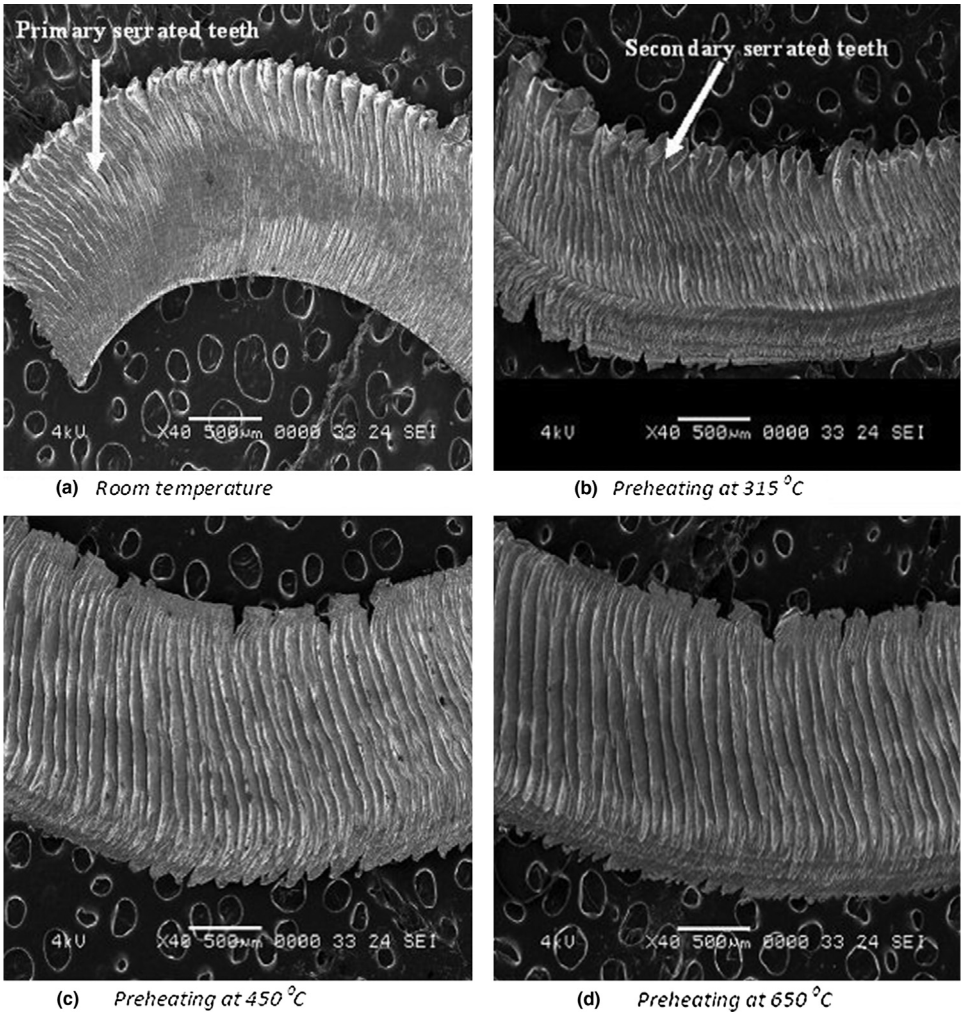

Figure 46 Chip produced in various runs at different temperature in end milling with uncoated WC–Co inserts for the same cutting condition at: (a) Room temperature; (b) 315 °C; (c) 450 °C; (d) 650 °C (cutting speed = 70 m min^{-1}, axial DOC = 1 mm, feed = 0.088 mm per tooth). Reproduced from Turnad, L. G. Improvement of Machinability of Titanium Alloy Ti-6Al-4V through Workpiece Preheating. Ph.D. Thesis, Manufacturing and Materials Engineering Department, IIUM, Malaysia, 2009.

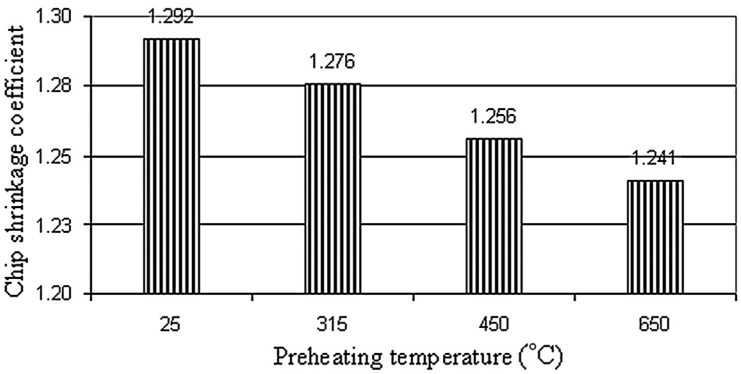

Figure 47 Chip shrinkage coefficients versus heating temperature (cutting speed = 70 m min^{-1}, feed = 0.088 mm per tooth, axial DOC = 1 mm, insert: uncoated WC–Co). Reproduced from Turnad, L. G. Improvement of Machinability of Titanium Alloy Ti-6Al-4V through Workpiece Preheating. Ph.D. Thesis, Manufacturing and Materials Engineering Department, IIUM, Malaysia, 2009.

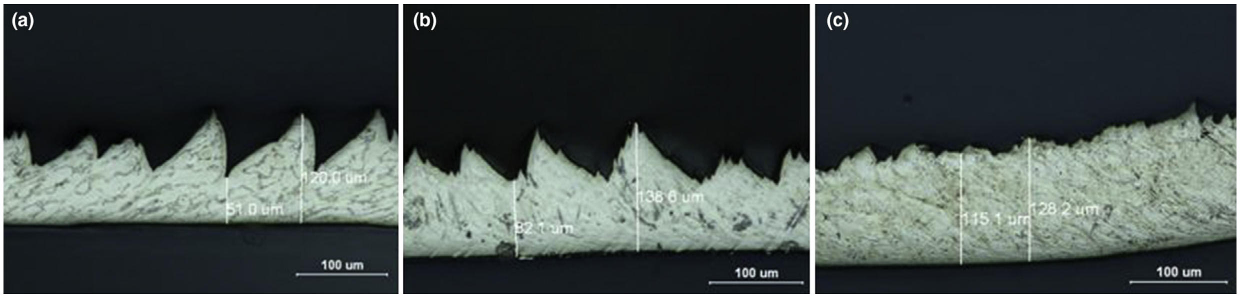

Figure 48 Cross-section of chips produced in machining using the same set of parameters but at different temperature: (a) Room temperature; (b) 450 °C; (c) 650 °C (cutting speed = 70 m min^{-1}, f_z = 0.088 mm per tooth, axial DOC = 1 mm, insert: uncoated WC–Co).

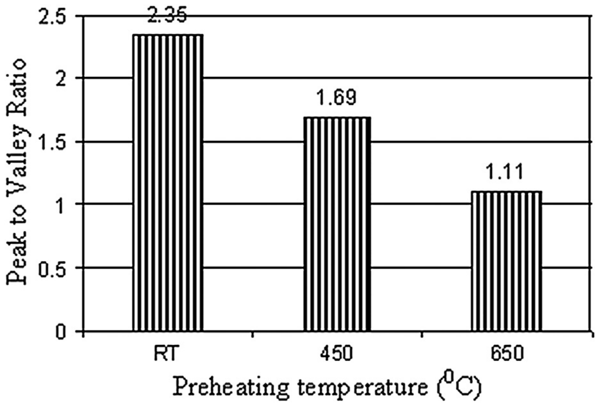

Figure 49 Peak to valley ratio versus heating temperature (cutting speed = 70 m min^{-1}, feed = 0.088 mm per tooth, and axial DOC = 1 mm, insert: uncoated WC–Co). Reproduced from Turnad, L. G. Improvement of Machinability of Titanium Alloy Ti-6Al-4V through Workpiece Preheating. Ph.D. Thesis, Manufacturing and Materials Engineering Department, IIUM, Malaysia, 2009.

machining, while, 127.8 min in tool life and 109.7 cm^3 in VMR were achieved in heat-assisted machining at 650 °C under the same cutting speed. The improvement of the tool life may be explained from several perspectives. Induction heating substantially decreases the resultant cutting force. Lower cutting force is attributed to the lower yield strength of the workpiece material at the elevated temperature. Thus, in heat-assisted machining, the shear stress reduces and contributes to lower the cutting forces. Heat-assisted machining also helps to ease the chip flow, which reduces frictional forces in the rake and flank faces of the tool. For instance, a decrease in cutting force by approximately 60% was recorded during heat-assisted machining at 650 °C, with uncoated WC–Co inserts at the cutting speed of 70 m min^{-1}. This result indicates the overwhelming benefits of using induction heating.

Suppression of chatter/vibration during heat-assisted machining is another advantage. The results of the experiments on the effects of heating temperature on chatter/vibration during cutting show that noticeable suppressions of chatter/vibration take place when heating is employed. For instance, a chatter/vibration was suppressed up to 88.2% during heat-assisted machining with uncoated WC–Co inserts at heating temperature of 650 °C. It substantiates the idea that heat-assisted machining can be utilized to eliminate chatter in machining. A reduced chatter/vibration eventually reduces the bouncing effect on the tool tip, and consequently, reduces the tool wear rates.

An increased chip-tool contact length due to the heating is also attributable to an increase in tool life. For instance, increased chip-tool contact length in 2.3 times was achieved when employing heating at temperature of 450 °C. Longer chip-tool contact length decreases the shear stress and the temperature close to tool tip. Those various factors play favorable roles and eventually reduce tool wear, and, consequently, increase tool life.

11.13.8.9 Summary

The investigation on the machinability of uncoated WC–Co and PCD inserts in the end milling of Ti–6Al–4V alloy has been extensively conducted under room temperature and heat-assisted conditions. The machinability assessment provides a comparison between room temperature and heat-assisted conditions. The evaluation includes tool life and tool wear morphology, surface roughness and surface integrity, cutting force, acceleration amplitude of vibration/chatter, chip-tool contact length, and chip morphology. Heat-assisted machining is found to help substantially reduce the tool wear rate, as well as increase tool life and volume of metal removal in the machining of Ti–6Al–4V alloy. This notable improvement in terms of tool life and volume of metal removal are explained as follows. Heat-assisted machining helps substantially soften the workpiece prior to cutting, which decreases the resultant cutting force. Lower cutting force and longer chip-tool contact length reduces the stresses acting on the cutting edge, and consequently decreases the tool wear rate. Suppression of vibration/chatter was also responsible for increasing tool life during heat-assisted machining as a result of lower dynamic stresses acting on the tool. Heat-assisted machining also significantly contributes to increase the chip-tool contact length. This aspect is important because of the shifting of the hot spot away from the cutting edge. The stresses acting on the tool are lowered, which leads to longer tool life. Heat-assisted machining also leads to a reduction in the chip serration frequency. A thin and long continuous chip produced during heat-assisted machining substantially helps reduce the cutting force, lowering the cutting pressure and cutting temperature.

Heat-assisted machining is also found to eliminate the effects of strain hardening during cutting. Results from microhardness measurement beneath the machined surface convincingly proved that the strain hardening caused by room temperature machining was sufficiently reduced by employing heating. In the subsurface investigation, three main zones beneath the top surface in cutting this alloy – heat-affected zone, strained hardening zone, and base metal zone – were identified. These zones are highly affected by the temperature employed during cutting.

Lastly, heat-assisted machining was found to appreciably improve the surface roughness, which eliminates the need for grinding and polishing operations. As a conclusion, heat-assisted machining with induction heating has been successfully proved to be an alternative method in increasing tool life, enhancing the volume of metal removal, and achieving a good surface finish in the end milling of titanium alloy Ti–6Al–4V with uncoated WC–Co. Thus, the improved machinability of titanium alloy Ti–6Al–4V through workpiece heating has been successfully established.

Finally, in all the cutting conditions and applications, including turning and end milling of the different work materials, application of heat-assisted machining has been proved to be a more beneficial method for improving the machinability of plain-carbon steel, heat-resistant and stainless steel, titanium alloys, and even hardened steels and alloys.

11.13.9 Conclusion

For successful application of heat-assisted or hot machining, reduction of strength of the material layer being removed needs to be achieved through localized and controlled heating of the work material within the machining zone. The heat is generally applied online during the machining process, but it can also be applied immediately prior to machining. The optimum heating temperature, at which maximum benefit of heat-assisted machining can be derived, is different for different materials and is close to the temperature at which the strength of the materials starts to decline abruptly.

Machinability enhancement of difficult-to-cut metals and alloys, as a result of application of external heat, is manifested in substantial reduction of cutting force and chatter amplitude and improved tool life, surface finish, and chip flow over the tool. Increases in chip-tool contact length, reduction of chip serration, and chatter amplitude achieved in heat-assisted machining facilitate reduced dynamic loading on the tool and lower intensity of tool wear and subsequently higher tool life. Lower surface roughness values attained in heat-assisted machining provide opportunities to cut down some of the inline finishing operations, such as grinding and rough polishing, which apparently would result in reduced machining lead time and consequently lower machining cost.

Subsurface investigations revealed that the strain-hardened layer produced in conventional room temperature machining is completely or partially eliminated during heat-assisted machining and would make it easier to remove the subsequent material layer and reduce the notch wear related to the strain-hardened layer.

References

1. Copley, S. M. Laser Shaping of Materials, Lasers in Materials Processing. In *Conference Proceedings of the American Society for Metals*, Los Angeles, CA, 1983, pp 82–92.
2. Konig, W.; Wagemann, A. Machining of Ceramic Components: Process-Technological Potentials. In *Machining of Advanced Materials*, NIST Special Publication, 1990, Vol. 847, pp 3–16.
3. Talantov, N. V.; Amin, A. K. M. N.; Chereomushnikov, N. P. Temperature Deformation Laws of Chatter Formation during Metal Cutting Process. In *Abstracts of the papers presented at the 5th Soviet National Conference, Teplophysika Technologichieskikh Processov*, Volgograd, 1980, p 92.
4. Amin, A. K. M. N.; Talantov, N. V. Influence of the Instability of Chip Formation and Preheating of Work on Tool Life in Machining High Temperature Resistant Steel and Titanium Alloys. *Mech. Eng. Res. Bull.* **1986,** *9*, 52–62.
5. Amin, A. K. M. N.; Abdelgadir, M. Control of Chatter Arising during Machining on Vertical Machining Center and Improvement of Tool Life and Surface Finish of the Machined Part by Preheating of the Workpiece by Induction Heating. Malaysia Patent MY-126082-A, 1982.
6. Amin, A. K. M. N.; Abdelgadir, M. The Effect of Preheating of Work Material on Chatter during End Milling of Medium Carbon Steel Performed on a Vertical Machining Center. *J. Mater. Sci. Eng. Trans. ASME, USA* **2003,** *125*, 667–680.
7. Amin, A. K. M. N.; Abraham, I.; Khairusshima, N. Performance of Circular Carbide Inserts in End Milling of Carbon Steel Under Preheating Condition. In *Proceedings of the ICAMT*, 2004, pp 65–73.
8. Amin, A. K. M. N.; Abdelgadir, M.; Kamaruddin, K. Effect of Workpiece Preheating on Machinability of Titanium Alloy. In *Proceedings of the International Conference ICAMT*, 2004, pp 145–152.
9. Klocke, F.; Zaboklicki, A. Innovation in der Umformtechnik – Laserunterstützte Verfahren. In *Blech Rohre Profile*, 1995, pp 383–343.
10. Gesellschaft, V. D. I.; Produktionstechnik, A. D. B. *Materialbearbeitung mit dem Laserstrahl im Geräte- und Maschinenbau;* VDI-Verlag: Düsseldorf, 1990.
11. Brecher, C.; Rosen, C. J.; Emonts, M. Laser-Assisted Milling of Advanced Materials. *Phys. Procedia* **2010,** *5*, 259–272.
12. Uehara, K.; Takeshita, H. Cutting Ceramics with a Technique of Hot Machining. *Ann. CIRP* **1986,** *35* (1), 55–58.
13. Amin, A. K. M. N.; Dolah, S.; Mahmud, M.; Lajis, M. A. Effects of Workpiece Preheating on Surface Roughness, Chatter and Tool Performance during End Milling of AISI D2 Tool Steel. *J. Mater. Process. Technol.* **2008,** *201*, 466–470.

14. Kok, P. Y.; Amin, A. K. M. N.; Faris, A. I. Performance of Preheating, Cryogenic Cooling and Combined Approaches in Improving Machinability of Stainless Steel in Turning. In *Proceedings of International Conference on Mechanical Engineering – ICME*, Dhaka, 2005, 34(1–5).
15. Leshock, Carl, E; Kim, Jin-Nam; Shin, Yung, C. Plasma Enhanced Machining of Inconel 718: Modeling of Workpiece Temperature with Plasma Heating and Experimental Results. *Int. J. Mach. Tools Manuf.* **2001,** *41,* 877–897.
16. Madhavulu, G.; Ahmed, B. Hot Machining Process for Improved Metal Removal Rates in Turning Operations. *J. Mater. Process. Technol.* **1994,** *44,* 199–206.
17. Steen, W. *Laser Material Processing,* 3rd ed.; Springer: New York, 2003.
18. Sun, S.; Brandt, M.; Dargusch, M. S. *Thermally Enhanced Machining of Hard-to-Machine Materials – A Review. Int. J. Mach. Tools Manuf.* **2010,** *50,* 2010, 663–680.
19. Dumitrescu, P.; Koshy, P.; Stenekes, J.; Elbestawi, M. A. High-Power Diode Laser Assisted Hard Turning AISI D2 Tool Steel. *Int. J. Mach. Tools Manuf.* **2006,** *46,* 2009–2016.
20. Rozzi, J. C.; Pfefferkorn, F. E.; Incropera, F. P.; Shin, Y. C. Transient Thermal Response of Rotating Cylindrical Silicon Nitride Workpiece Subjected to Translating Laser Heat Source, Part I: Comparison of Surface Temperature Measurements with Theoretical Results. *J. Heat Transfer Trans. ASME* **1998,** *120,* 899–906.
21. Pfefferkorn, F. E.; Incropera, F. P.; Shin, Y. C. Heat Transfer Model of Semi-Transparent Ceramics Undergoing Laser-Assisted Machining. *Int. J. Heat Mass Transfer* **2005,** *48,* 1999–2012.
22. Wu, X.; Zhang, H.; Wang, Y. Three-Dimensional Thermal Analysis for Laser Assisted Machining of Ceramics Using FEA. In *Proceedings of SPIE, Fourth International Symposium on Advanced Optical Manufacturing and Testing Technologies: Advanced Optical Manufacturing Technologies*, Vol. 7282, 2009, pp 72822I-1–72822I-5.
23. Wu, J. F.; Guu, Y. B. Laser Assisted Machining Methods and Device, US Patent 7,002,100 B2, 2004.
24. Weck, M.; Zeppelin, W. V.; Hermanns, C. Laser – A Tool for Turning Centers. In *Laser Assisted Net Shape Engineering, Proceedings of the LANE'94.* Vol. 1; Geiger, M., Vollertsen, F., Eds.; Meisenbach: Bamberg, 1994; pp 427–437.
25. Rajagopal, S.; Plankenhorn, D. J.; Hill, V. L. Machining Aerospace Alloys with the Aid of a 15kW Laser. *J. Appl. Metalwork.* **1982,** *2,* 170–184.
26. Sun, S.; Harris, J.; Brandt, M. Parametric Investigation of Laser-Assisted Machining of Commercially Pure Titanium. *Adv. Eng. Mater.* **2008,** *10,* 565–572.
27. Anderson, M.; Patwa, R.; Shin, Y. C. Laser-Assisted Machining of Inconel 718 with an Economic Analysis. *Int. J. Mach. Tools Manuf.* **2006,** *46,* 1879–1891.
28. Ding, H.; Shin, Y. C. Laser-Assisted Machining of Hardened Steel Parts with Surface Integrity Analysis. *Int. J. Mach. Tools Manuf.* **2010,** *50,* 106–114.
29. Shin, Y.C. Laser Assisted Machining Process with Distributed Lasers. US Patent 0062920A1, 2007.
30. Salem, W. B.; Marot, G.; Moisan, A.; Longuemard, J. P. Laser Assisted Turning during Finishing Operation Applied to Hardened Steels and Inconel 718. In *Laser Assisted Net Shape Engineering, Proceedings of the LANE'94.* Vol. 1; Geiger, M., Vollertsen, F., Eds.; Meisenbach: Bamberg, 1994; pp 455–464. Proceedings of the LANE'94.
31. Armitage, K. Laser Assisted Machining of High Chromium White Cast Iron. Thesis for Master of Engineering, Swinburne University of Technology, 2005.
32. Walter, J.; Ritzi, R. Increasing Tool Life by Laser Assisted Turning. In *Laser Assisted Net Shape Engineering 4, Proceedings of the LANE 2004,* Vol. 2; Geiger, M., Otto, A., Eds.; Meisenbach: Bamberg, 2004; pp 1157–1164.
33. Yang, B.; Lei, S. Laser-Assisted Milling of Silicon Nitride Ceramic: A Machinability Study. *Int. J. Mechatron. Manuf. Syst.* **2008,** *1,* 116–130.
34. Lacalle, L. N. L. D.; Sanchez, J. A.; Lamikiz, A.; Celaya, A. Plasma Assisted Milling Heat-Resistant Superalloys. *J. Manuf. Sci. Eng. Trans. ASME* **2004,** *126,* 274–285.
35. Thomas, T.; Vigneau, J. O. Laser-Assisted Milling Process. US Patent 5,906,459, 1999.
36. Konig, W. K.; Zaboklicki, A. K. Laser-Assisted Hot Machining of Ceramics and Composite Materials. In *International Conference on Machining of Advanced Materials*, NIST Special Publication, Gaithersburg, MD, 1993, Vol. 847, pp 455–463.
37. Demmer, A.; Bausch, S.; Groll, K. Perspectives for Laser-Assisted Machining: Cost-Effective Processing of Difficult-to Machine Materials. *Ind. Laser User* **2005,** 38–41.
38. Tian, Y.; Wu, B.; Anderson, M.; Shin, Y. C. Laser-Assisted Milling of Silicon Nitride and Inconel 718. *J. Manuf. Sci. Eng. Trans. ASME* **2008,** *130,* 031013-1–031013-9.
39. Komanduri, R.; Flom, D. G.; Lee, M. Highlights of DARPA Advanced Machining Research Program. In *American Society of Mechanical Engineers, Production Engineering Division (Publication) PED 12*, 1984; pp 15–36.
40. Konig, W.; Zaboklicki, U. Laser-Assisted Hot Machining of Ceramics and Composite Materials. In *Machining of Advanced Materials*, NIST Special Publication, 1993, Vol. 847, pp 455–463.
41. Chryssolouris, G.; Anifantis, N.; Karagiannis, S. Laser Assisted Machining: An Overview, 75th anniversary Issue. *J. Manuf. Sci. Eng. Trans. ASME* **1997,** *119,* 766–769.
42. Amin, A. K. M. N. Investigation of the Laws Governing the Formation of Chatter during Metal Cutting Processes and their Influence on Tool Wear. Ph.D. Thesis (in Russian), Volgograd Polytechnic Institute, Volgograd, Russia, 1982.
43. Trent, E. M. *Metal Cutting,* 3rd ed.; Butterworths Publishing Company: UK, 2000.
44. Turnad, L. G. Improvement of Machinability of Titanium Alloy Ti-6Al-4V through Workpiece Preheating. Ph.D. Thesis, Manufacturing and Materials Engineering Department, IIUM, Malaysia, 2009.
45. Amin, A. K. M. N.; Abdelgadir, M. The Effect of Preheating of Work Material on Improved Machinability of Materials. In *Proceedings of the International Conference AIMTDR*, Ranchi, India, 2002.
46. Main Catalogue, Sandvik Coromat, 2006.